CAMERA ELECTRONICS FOR LOW-COST MICROBOLOMETER TYPE INFRARED DETECTORS

A THESIS SUBMITTED TO
THE GRADUATE SCHOOL OF NATURAL AND APPLIED SCIENCES
OF
MIDDLE EAST TECHNICAL UNIVERSITY

BY

CEREN TÜFEKÇİ

IN PARTIAL FULFILLMENT OF THE REQUIREMENTS
FOR
THE DEGREE OF MASTER OF SCIENCE
IN
ELECTRICAL AND ELECTRONICS ENGINEERING

JANUARY 2013

Approval of the thesis:

CAMERA ELECTRONICS FOR LOW-COST MICROBOLOMETER TYPE INFRARED DETECTORS

submitted by **CEREN TÜFEKÇİ** in partial fulfillment of the requirements for the degree of **Master of Science in Electrical and Electronics Engineering Department, Middle East Technical University** by,

Prof. Dr. Canan Özgen
Dean, Graduate School of **Natural and Applied Sciences** _____

Prof. Dr. İsmet Erkmen
Head of Department, **Electrical and Electronics Engineering** _____

Prof. Dr. Tayfun Akın
Supervisor, **Electrical and Electronics Eng. Dept., METU** _____

Dr. Selim Eminoğlu
Co-Supervisor, **Mikro-Tasarım Ltd. Şti.** _____

Examining Committee Members:

Assoc. Prof. Dr. Haluk Külah
Electrical and Electronics Engineering Dept., METU _____

Prof. Dr. Tayfun Akın
Electrical and Electronics Engineering Dept., METU _____

Assoc. Prof. Dr. Barış Bayram
Electrical and Electronics Engineering Dept., METU _____

Dr. Selim Eminoğlu
Mikro-Tasarım Ltd. Şti. _____

Dr. Selçuk Özer
Aselsan A.Ş. _____

Date: 30.01.2013

I hereby declare that all information in this document has been obtained and presented in accordance with academic rules and ethical conduct. I also declare that, as required by these rules and conduct, I have fully cited and referenced all material and results that are not original to this work.

Name, Last Name: Ceren Tüfekçi

Signature

ABSTRACT

CAMERA ELECTRONICS FOR LOW-COST MICROBOLOMETER TYPE INFRARED DETECTORS

Tüfekçi, Ceren

M. Sc., Department of Electrical and Electronics Engineering

Supervisor: Prof. Dr. Tayfun Akın

Co-Supervisor: Dr. Selim Eminoğlu

January 2013, 72 pages

This thesis presents a study on the design and development of camera electronics for low cost microbolometer type infrared detectors. Two camera modules are designed and realized in the scope of this thesis; 1) portable camera module which aims to be a compact and low cost, and 2) miniature camera module which is optimized to have minimum volume with best performance.

The portable camera module enables hand-held infrared imaging with its reduced size which is 7.5×5 cm^2. The module contains a sensor interface board, camera electronics board, and digital interface and USB communication board. The overall module is powered by an external 6 V supply and directly connected to a host computer via USB interface. The test results of the realized portable camera module shows that the power dissipation of the overall camera module is less than 0.6 W and the system noise is less than 0.44mV_{RMS}.

The miniature camera carries the portable camera concept one step further in order to achieve an ultra-portable and USB powered infrared camera system.The reduced size of the miniature camera, which is 2.9×2.9 cm^2, dictates that both the electronics and the mechanical design of the miniature camera are critically important. The miniature camera module contains a sensor interface board, a power board, a digital interface board, and a USB communication board. The module is powered by the USB interface and does not require any additional power sources. The test results of the realized miniature camera system shows that the power dissipation of the overall module is 0.55 W, and the system noise is less than 80 μV_{RMS}.

The miniature camera module designed and realized in the scope of this thesis is the first miniature infrared camera module in Turkey. The developed camera modules can be used to produce very low cost and ultra-portable infrared camera systems.

Keywords: Infrared camera electronics, low-cost microbolometers, miniature camera system, portable camera system, USB powered camera electronics

ÖZ

DÜŞÜK MALİYETLİ MİKROBOLOMETRE TİPİ KIZILÖTESİ DEDEKTÖRLER İÇİN KAMERA ELEKTRONİĞİ

Tüfekçi, Ceren

Yüksek Lisans, Elektrik ve Elektronik Mühendisliği Bölümü

Tez Yöneticisi: Prof. Dr. Tayfun Akın

Ortak Tez Yöneticisi: Dr. Selim Eminoğlu

Ocak 2013, 72sayfa

Bu tezde düşük maliyetli mikrobolometre tipi kızılötesi dedektörler için kamera elektroniği tasarımı ve geliştirilmesi üzerine yapılan bir çalışma sunulmaktadır. Tez kapsamında iki kamera modülü tasarlanıp gerçekleştirilmiştir: 1) kompakt ve düşük maliyetli taşınabilir kamera modülü, 2) yüksek performanslı ve minimum hacimli minyatür kamera modülü.

Taşınabilir kamera modülü $7.5 \times 5\ cm^2$ boyutunda olup, elde taşınabilir kızılötesi görüntülemeye olanak sunmaktadır. Modül, sensor arayüz kartı, kamera elektroniği kartı ve dijital arayüz ve USB haberleşme kartlarını kapsamaktadır. Modül, harici 6V kaynak ile güçlendirilmekte ve USB arayüzü aracılığıyla ana bilgisayara bağlanmaktadır. Taşınabilir kamera modülünün test sonuçları güç kullanımının 0.6W ve sistem gürültüsünün $0.44mV_{RMS}$ oldugunu göstermektedir.

Minyatür kamera, taşınabilir kamera anlayışının bir adım daha ileri götürülmesi ile elde edilen kolay taşınabilir ve USB arayüzünden güçlendirilen bir kızılötesi kamera sistemidir. Minyatür kameranın boyutu $2.9 \times 2.9\ cm^2$ olup, kameranın elektronik ve mekanik tasarımını önemli hale getirrmiştir. Minyatür kamera modülü, sensor arayüz kartı, güç kartı, dijital arayüz kartı ve USB haberleşme kartlarını kapsamaktadır. Modül, USB arayüzden güçlendirilmektedir ve herhangi bir ek güç kaynağına gerek duymamaktadır. Minyatür kameranın test sonuçları güç kullanımının 0.55W ve sistem gürültüsünün $80\mu V_{RMS}$ oldugunu göstermektedr.

Bu tez kapsamında tasarlanan ve gerçekleştirilen minyatür kamera modülü, Türkiye'de yapılan ilk minyatür kızılötesi kamera modülüdür. Geliştirilen kamera modülleri düşük maliyetli ve kolay taşınabilir kızılötesi kamera sistemlerinde kullanılabilir.

Anahtar kelimeler: Kızılötesi kamera elektroniği, düşük maliyetli mikrobolometreler, minyatür kamera sistemi, taşınabilir kamera sistemi, USB'den güçlendirilen kamera elektroniği

To my family

ACKNOWLEDGMENT

I would like to express my appreciation to my advisor Prof. Dr. Tayfun Akın for his supervision and guidance throughout this study. It is an opportunity to work with him. Iwould like to thank Dr. Selim Eminoğlu for his endless support and trust through my graduate life. I would like to thank Dr. Murat Tepegöz for his invaluable assistance and guidance for this study.

I would like to thank Alperen Toprak and Dinçay Akçören for their guidance and sharing their knowledge and experience.

I would like to thank Alper Küçükkömürler and Fırat Tankut for their valuable suggestions during the design and test of the designed cameras. I would also thank Cavid Musayev, Zafer Zamboğlu, Nihan Eminoğlu for providing a pleasant working environment and their support.

I would like to thank Şeniz Esra Küçük for her friendship and help in the writing cycle of thisthesis.

I would like to thank Güneş Özuygun and Boğaç Saral for their invaluable friendship through secondary school years. I would like to thank Gönül Ünal and Güneş Uyanıksoy for their friendship and support through my undergraduate years. I would like to thank Selçuk Doğan for his endless support and patience. I would like to thank Onur Şimşek, Deniz Onay, and Volkan Atmaca for their friendship.

I would like to thank Burak Eminoglu, Başak Kepapçı, Sevil Zeynep Lüleç, Andaç Lüleç, Tuncer Askerli, Şükrü Ufuk Şenveli, İlker Ender Ocak, Mert Torunbalcı, Onur Yalçın, Soner Sönmezoğlu, Selçuk Keskin, Numan Eroğlu, Osman Aydın, Serdar Tez, and Erdinç Tatar for their invaluable friendship.

I would like to thank to all members of the METU-MEMS, BIO-MEMS and RF-MEMS research groups for providing a friendly environment.

At last but not least, I would like to thank my father, my mother, and my sister for their endless trust, encouragement, and patience in every moment of my life. Without their invaluable support, I would not achieve this success. I would like to thank my aunt-homemate for her hospitality and support through my life. I would like to thank my uncle Atilla and my cousin Doruk for their support.

TABLE OF CONTENTS

ABSTRACT ..... **v**

ÖZ ..... **vi**

ACKNOWLEDGMENT ..... **viii**

LIST OF FIGURES ..... **xi**

LIST OF TABLES ..... **xiv**

CHAPTERS

1 INTRODUCTION **1**

1.1 Imaging systems 1

1.2 Infrared Imaging System 2
1.2.1 Infrared Detectors 2
1.2.2 Infrared Camera 4

1.3 Low Cost Infrared Sensors and Camera 8
1.3.1 Sensor Introduction 10
1.3.2 Performance Parameters of Low Cost Uncooled Microbolometer 12

1.4 Research Objectives and Organization of the Thesis 13

2 CAMERA DESIGN FOR LOW COST UNCOOLED MICROBOLOMERS **15**

2.1 Introduction 15

2.2 Design Guidelines for High Performance Camera Electronics 15
2.2.1 Crosstalk 16
2.2.2 Power and Ground Routings 16
2.2.3 Supply Decoupling 18
2.2.4 Ground Bounce 18
2.2.5 Board to Board Connections 19
2.2.6 USB Powered Devices 19
2.2.7 Analog Signal Flow 19

2.3 Previous Works on Camera Design in METU 20

2.4 Design Cycle of the Portable and Miniature Camera Development 22

2.5 Portable Camera Electronics 24
2.5.1 Sensor Interface Board 24
2.5.2 Camera Electronics Board 25
2.5.3 Digital Interface and USB Communication Board 28

2.6 Miniature Camera Electronics 30
2.6.1 Miniature Sensor Interface Board 31
2.6.2 Miniature Power Board 34
2.6.3 Miniature Digital Interface Board 35
2.6.4 Miniature USB Communication Board 36

2.7 Camera Board Design 37

2.7.1 Board Layers 37
2.7.2 Ground and Power Distribution 45
2.8 Conclusion 48

3 IMPLEMENTATION 49
3.1 Introduction 49
3.2 Mechanical Design 49
3.2.1 Mechanical Design of the Portable Camera 49
3.2.2 Mechanical Design of the Miniature Camera 51
3.3 Housing and Optics 52
3.4 Conclusion 54

4 TEST RESULTS 55
4.1 Introduction 55
4.2 Portable Camera 56
4.3 Miniature Camera 60
4.4 Conclusion 68

5 CONCLUSION AND FUTURE WORK 69

6 REFERENCES 71

LIST OF FIGURES

FIGURES

Figure 1.1: Atmospheric transmission characteristics of the infrared portion in the electromagnetic spectrum [2]. 2
Figure 1.2: Representative perspective view of a microbolometer detector [6, 7]. 4
Figure 1.3: Photograph of Evaporograph. In 1929, Hungarian physicist Kálmán Tihanyi invented an IR-sensitive electronic camera for anti-aircraft defense [15]. 5
Figure 1.4: A “portable” infrared radiometer used to measure infrared scene profiles at Syracuse University in the late 1950’s [17]. 6
Figure 1.5: First portable infrared camera developed by FLIR systems in 1960’s [18]. 6
Figure 1.6: First portable infrared camera with 240×236 microbolometer is produced by Honeywell in 1990 [19]. 7
Figure 1.7: A compact microbolometer type infrared camera with 240×340 FPA size produced by Amber Engineering Inc. in 1995 [19]. 7
Figure 1.8: Applications of the infrared imaging [39]. 8
Figure 1.9: Uncooled thermal camera business (units) [16]. 9
Figure 1.10: FLIR Quark uncooled core [37]. 9
Figure 1.11: Photograph of a fabricated die of 160×120 uncooled thermal sensor. 11
Figure 2.1: The middle layer of the power board of the miniature camera. 16
Figure 2.2: Star grounding scheme. 17
Figure 2.3: Grounding of mixed signal circuits. 17
Figure 2.4: Representative view of grounding of the ROIC and ADC in the designed camera electronics. 18
Figure 2.5: Block diagram of the analog signal block. 20
Figure 2.6: Test setup for the low cost microbolometer camera used in earlier studies [20]. 20
Figure 2.7: An image taken with 160×120 microbolometer and dewar setup [20]. 21
Figure 2.8: Photograph of the handheld camera. 22
Figure 2.9: Design cycle of the camera electronics. 23
Figure 2.10: Block diagram of the portable camera. 24
Figure 2.11: Block diagram of the camera electronics board of the portable camera. 25
Figure 2.12: Power block diagram of the camera electronics board. 26
Figure 2.13: Digital level translator block diagram of the camera electronics board. 26
Figure 2.14: Analog signal block of the portable camera electronics. 27
Figure 2.15: Block diagram of the digital interface and USB communication board. 28
Figure 2.16: Block diagram of the miniature camera. 31
Figure 2.17: Block diagram of the miniature sensor interface board. 31
Figure 2.18: Analog signal block of the miniature camera. 32
Figure 2.19: Spice simulation result of the LT6350 single ended to differential converter. Common mode signal of the converter (vcm), analog output signal of the detector (vin), the first output of the converter (out1), the second output of the converter (out2) indicated by pink, green blue, and red, respectively. “out1” and “out2” signals are the input signals of the ADC (LTC2379), and they are fully differential with respect to “vcm”. 33
Figure 2.20: Block diagram of the power board of the miniature camera. 34
Figure 2.21: Block diagram of the miniature digital interface board. 35
Figure 2.22: Block diagram of the USB communication board. 36
Figure 2.23: Block diagram of the (a) top side, (b) bottom side of the sensor interface board of the portable camera. 38
Figure 2.24: Photograph of the (a) top side, (b) bottom side of the sensor interface board of the portable camera. 38

Figure 2.25: Block diagram of the (a) top side, (b) bottom side of the camera electronics board of the portable camera. 39
Figure 2.26: Photograph of the (a) top side, (b) bottom side of the camera electronics board of the portable camera. 39
Figure 2.27: Block diagram of the (a) top side, (b) bottom side of the digital interface and USB communication board of the portable camera. 40
Figure 2.28: Photograph of the (a) top side, (b) bottom side of the digital interface and USB communication board of the portable camera. 40
Figure 2.29: Block diagram of the (a) top side, (b) bottom side of the sensor interface board of the miniature camera. 41
Figure 2.30: Photograph of the (a) top layer, (b) bottom layer of the sensor interface board of the miniature camera. 41
Figure 2.31: Block diagram of the (a) top side, (b) bottom side of the power board of the miniature camera. 42
Figure 2.32: Photograph of the (a) top layer, (b) bottom layer of the power board of the miniature camera. 42
Figure 2.33: Block diagram of the (a) top side, (b) bottom side of the digital interface board of the miniature camera. 43
Figure 2.34: Photograph of the (a) top layer, (b) bottom layer of the digital interface board of the miniature camera. 43
Figure 2.35: Block diagram of the (a) top side, (b) bottom side of the USB communication board of the miniature camera. 44
Figure 2.36: Photograph of the (a) top layer, (b) bottom layer of USB communication board of the miniature camera. 44
Figure 2.37: Ground distribution of the portable camera electronics. 45
Figure 2.38: Power distribution of the portable camera electronics. 46
Figure 2.39: Ground distribution of the USB powered miniature camera electronics. 47
Figure 2.40: Power distribution of the miniature camera electronics. 48
Figure 3.1: Mechanical design of the portable camera. 50
Figure 3.2: Photograph of the portable camera. 50
Figure 3.3: Mechanical design of the miniature camera. 51
Figure 3.4: Photograph of the miniature camera. 52
Figure 3.5: Housing of the portable camera. The dimension of the housing is 7.9x5.4x2.2cm^3 without lens. 53
Figure 3.6: Housing of the miniature camera. The dimension of the housing is 3.1×3.1×3.1 cm^3 without lens. 53
Figure 4.1: Simplified block diagram of the readout electronics of the 160×120 microbolometer. 55
Figure 4.2: The test setup for the portable camera. The test setup consists of a low noise DC power supply, a computer, and the portable camera. 56
Figure 4.3: Signal chain noise histogram of the portable camera. The average noise is 2.9 ADC count with 14-bit ADC which corresponds to 0.44m V_{RMS}. 57
Figure 4.4: Zero gain noise histogram of the portable camera. The average noise is 3.1 ADC count with 14-bit ADC which corresponds to 0.47m V_{RMS}.. 58
Figure 4.5: Detector noise histogram of the portable camera. The average noise is 10.2 ADC counts with 14-bit ADC which corresponds to 1.56m V_{RMS}. 59
Figure 4.6: Test setup for the DC supply powered miniature camera. The test setup consists of a low noise DC power supply, a computer, and the miniature camera. 61
Figure 4.7: Test setup for the USB powered miniature camera. The test setup consists of a computer and the miniature camera. 61
Figure 4.8: Signal chain noise histogram of the miniature camera with supply power. The average noise is 1 ADC count with 18-bit ADC which corresponds to 19µ V_{RMS}. 62
Figure 4.9: Signal chain noise histogram of the miniature camera with USB power. The average noise is 1.2 ADC count with 18-bit ADC which corresponds to 23µ V_{RMS}. 63
Figure 4.10: Zero gain noise histogram of the miniature camera with supply power. The average noise is 4.3 ADC count with 18-bit ADC which corresponds to 0.08m V_{RMS}. 64
Figure 4.11: Zero gain noise histogram of the miniature camera with USB power. The average noise is 9.1 ADC count with 18-bit ADC which corresponds to 0.17m V_{RMS}. 65

Figure 4.12: Detector noise histogram of the miniature camera with supply power. The average noise is 185 ADC count with 18-bit ADC which corresponds to 3.53m V_{RMS}..... 66
Figure 4.13: Detector noise histogram of the miniature camera with USB power. The average noise is 190 ADC count with 18-bit ADC which corresponds to 3.62m V_{RMS}. 66
Figure 4.14: An image taken with the 160x120 microbolometer with miniature camera. 67

LIST OF TABLES

TABLES

Table 1.1: Features of the 160×120 microbolometer [23].....12
Table 2.1: Technical specifications of the portable camera. 30
Table 2.2: Technical specifications of the miniature camera. 37
Table 4.1: Features of the portable camera. 60
Table 4.2: Features of the miniature camera. 68

CHAPTER 1

INTRODUCTION

1.1 Imaging systems

Imaging systems are composed of two main parts: *the sensor* converting the image into electrical signals, and *the electronics* interpreting this electrical signal and forming the visual display. The sensor convertsthe incoming radiation to electrical signal.The external electronics read and process the sensor output signal and convert to the digital domain. Finally, the image is visualized with the use of dedicated hardware and software.

Electromagnetic radiation extends from low frequency radio waves to high frequency gamma rays. A detector usually senses a specific region of the electromagnetic spectrum. Human eye can see only the visible portion of the electromagnetic spectrum. The visible light covers the wavelengths from 390 nm to 750 nm, which is 400 THz to 790 THz in terms of frequency.Visible detectors sense that region of the electromagnetic spectrum. One of the most important electromagnetic radiation regions is the infrared region because all objects emit infrared radiation, if the absolute temperature of the object is higher than 0 K.Infrared detectors sense the infrared portion of the spectrum. Infrared radiation covers the wavelengths from 750 nm to 1mm in the electromagnetic spectrum. There are three sub-infrared regions in the spectrum. The electromagnetic region with the wavelength of 750 nm to 3 µm is called near infrared region, the electromagnetic region with the wavelength of 3 µm to 6 µm is called middle infrared region, and the electromagnetic region with the wavelength of 6 µm to 15 µm is called far infrared region. [1]

Atmospheric transmission characteristics are important for the selection of the detector type. Figure 1.1 shows the atmospheric transmission characteristics of the infrared portion in the electromagnetic spectrum [2]. There are atmospheric windows with the lower absorption in the transmittance of the infrared. 3 µm to 5 µm bandwidth is one of the transmission windows, and the other transmittance window is the 8 µm to 12 µm bandwidth. In these windows, loss due to the atmospheric absorption is negligible. Therefore, 3 µm to 5 µm bands and 8 µm to 12 µm bands are used in thermal imaging.

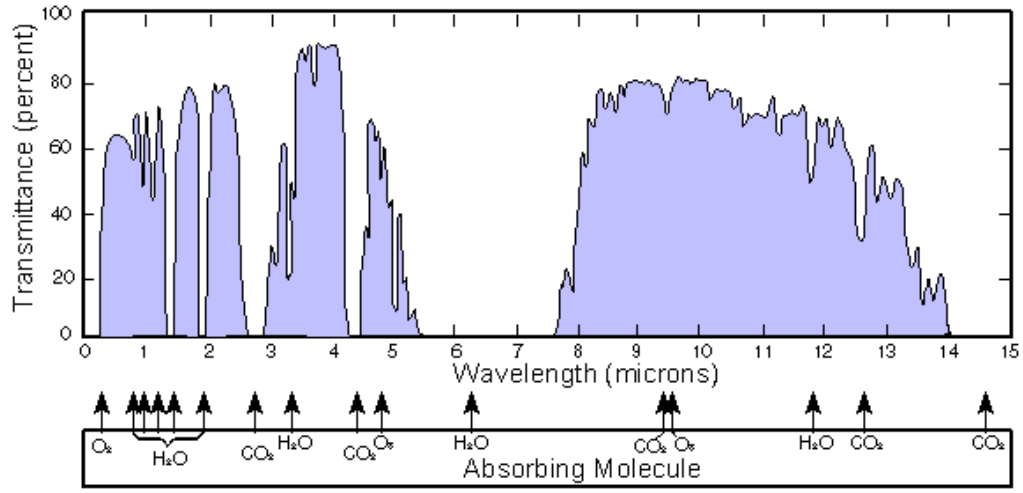


Figure 1.1: Atmospheric transmission characteristics of the infrared portion in the electromagnetic spectrum [2].

1.2 Infrared Imaging System

An infrared imaging system is composed of an infrared detector with the readout electronics, camera electronics, optics, and housing. The studies in this thesis focus on the camera electronics.

The readout electronics senses the detector output signal and converts it to an analog signal. The analog output signal of the readout electronics is sensed by the camera electronics. The camera electronics converts the analog signal to a digital signal using an ADC. Then, image is obtained from the digitized data with the help of the software.

Finally, the optical lens and housing parts of the system are used to focus the infrared radiation to the focal plane array (FPA) and to form the camera from the camera electronics boards, respectively.

1.2.1 Infrared Detectors

There are basically two types of infrared detectors: photon and thermal detectors. In the next sections, photon and thermal detectors will be discussed.

1.2.1.1 Photon Detectors

The photon detectors have faster response time and higher sensitivity than the thermal detectors. The photon detectors are based on the excitation of the electrons in a semiconductor as a result of the incoming infrared radiation.There is incident light to the surface of the detector. If the energy of the photon exceeds the bandgap energy of the semiconductor, electron-hole pairs are created. Therefore, low bandgap semiconductors are used to excite the electrons. Incident infrared

radiation can be measured by counting the number of the electron-hole pairs. The photon detectors must be cooled down to cryogenic temperatures to detect the small number of incident photons because there are many more thermally excited carriers than the incident photons at high temperatures[3].

1.2.1.2 Thermal Detectors

The second type of the infrared detectors is the thermal detectors which can operate at room temperature. Furthermore, these types of the detectors have low power consumption and are low-cost detectors. Thermal detectors operate on the principlethat the electrical properties of the active materials change with respect to the incoming infrared radiation [4]. The temperature difference can be interpreted from the electrical properties of the active materials. There are three types of the thermal detectors: thermopile detectors, pyroelectric detectors, and microbolometers.

1.2.1.2.1 Thermopile Detectors

Thermopile detectors are the type of the thermal detectors whose operation principle is the Seebeck effect.

Thermopile detectors are composed of two different conductive materials with different Seebeck coefficients joined at a single junction while the other ends are open. The incoming infrared radiation is absorbed at this junction, and the radiation starts to heat up these materials. Heat at the absorption region causes a temperature gradient between the two ends of the materials. Then, a voltage difference is generated between open ends of the materials due to the temperature gradient that is discovered by Thomas Johann Seebeck [5, 36].Thermopile detectors have lower responsivity than the other types of the thermal detectors.

1.2.1.2.2 Pyroelectric Detectors

The second type of the thermal detectors is pyroelectric detectors. These detectors are based on pyroelectricityproperty of materials. If there is an electric field, every material is polarized. However, even if there is no electric field, pyroelectric materials can be polarized simultaneously due to a change in temperature value. In other words, pyroelectricity is the generation of voltage when certain materials are heated or cooled.Positions of the atoms in the crystal structure are changed with the change in the polarization with respect to the temperature. Therefore, a voltage is generated due to this change.

1.2.1.2.3 Microbolometers

Microbolometersare based on the change in the electrical property of the active material due to the incoming infrared radiation. The incoming radiation is absorbed with an absorber layer and the radiation heats up the detector. The electronics embedded together with the detectors sense this heating up and converts it to an electrical signal. The electrical output of the sensor is processed and converted into an image format by camera electronics.

There are two types of microbolometers: the resistive type and the diode type microbolometers. In the resistive type microbolometers, the incoming infrared radiation is absorbed by the absorber layer then the temperature of the pixel increases. Figure 1.2 shows the representative perspective view of a microbolometer detector [6, 7]. Resistive microbolometers operate based on the temperature coefficient of resistance (TCR) of the active material. Resistance of the active material changes with respect to the TCR of the material.

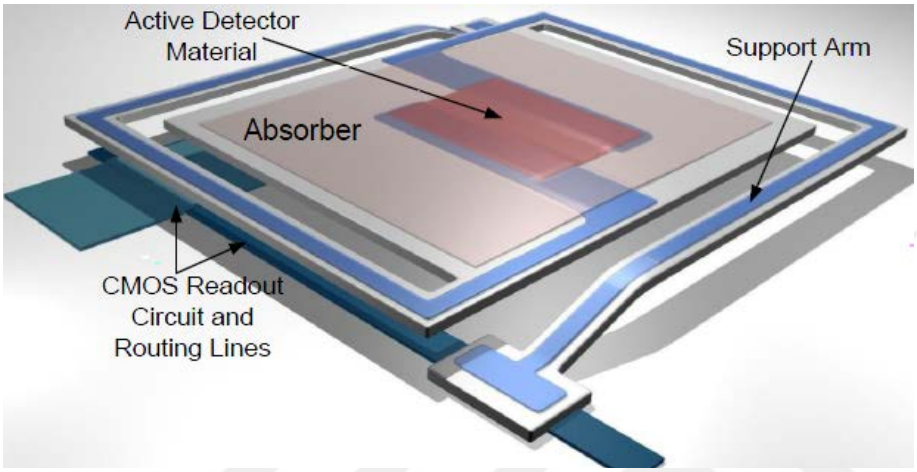


Figure 1.2: Representative perspective view of a microbolometer detector[6, 7].

In the diode type microbolometers, the sensing element is a diode. This type of microbolometer is based on the forward voltage or current of the diodes and the change in the forward voltage or current is measured.

Resistive type microbolometers are designed and produced in the METU-MEMS Reseach and Applications Center for years. Diode type microbolometers have low performance, but very easy fabrication process compared to the resistive type microbolometers. Therefore these type of the microbolometers are used for low cost imagery [8, 9, 10, 11, 12, 13, 14].

1.2.2 Infrared Camera

An infrared camera creates images out of tiny temperature differences detected by infrared sensors. Infraredcamera generates images that cannot be seen by eyes. The infrared camera includes the infrared detector with the ROIC (Readout Integrated Circuit), the camera electronics to create an image, and a lens to focus the object.

Evaporograph, is the first conventional IR camera was declassified around 1956 [15]. Figure 1.3 shows the picture of an Evaporograph. In 1929, Hungarian physicist Kálmán Tihanyi invented an IR-sensitive electronic camera for anti-aircraft defense [15]. It is also the first non-scanned IR imager. Infrared radiation is focused to the blackened membrane coated with thin film oil. Differential rate of the oil evaporation is proportional to the intensity of the radiation. Visible illumination is focused on to the same film to produce an interference pattern corresponding to the thermal image [16].

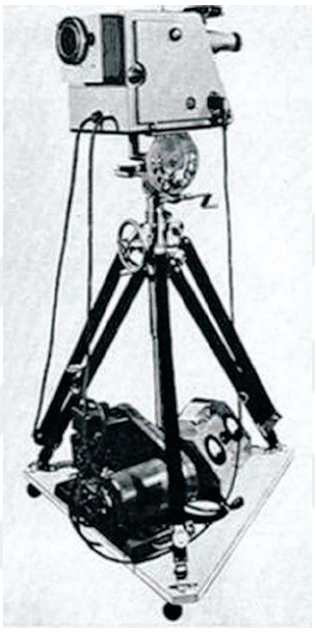


Figure 1.3: Photograph of Evaporograph. In 1929, Hungarian physicist Kálmán Tihanyi invented an IR-sensitive electronic camera for anti-aircraft defense [15].

Infrared imaging developments generally began in the 1950s. Figure 1.4 shows a "portable" infrared radiometer used to measure infrared scene profiles at Syracuse University in the late 1950's [17]. In early 1960's, FLIR developed a cooled portable night vision system. Figure 1.5 shows the first portable infrared camera developed by FLIR systems in 1960's [18].



Figure 1.4: A “portable” infrared radiometer used to measure infrared scene profiles at Syracuse University in the late 1950’s [17].



Figure 1.5: First portable infrared camera developed by FLIR systems in 1960’s [18].

Figure 1.6shows the first portable infrared camera with 240×236 microbolometer is produced by Honeywell in 1990 [19]. In addition, Figure 1.7shows A compact microbolometer type infrared camera with 240×340 FPA size produced by Amber Engineering Inc. in 1995 [19].

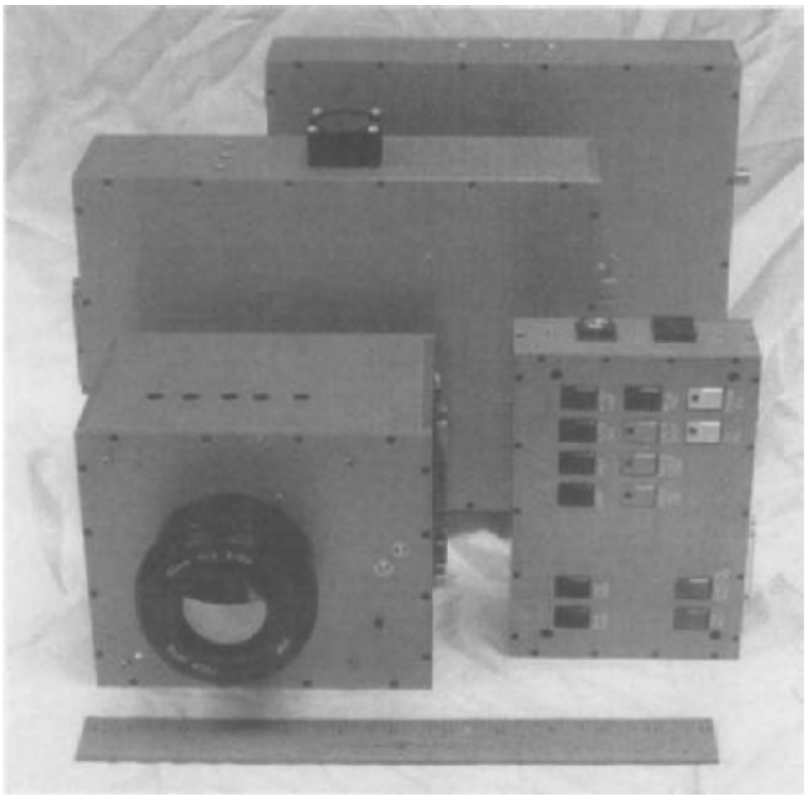


Figure 1.6: First portable infrared camera with 240×236 microbolometer is produced by Honeywell in 1990 [19].



Figure 1.7: A compact microbolometer type infrared camera with 240×340 FPA size produced by Amber Engineering Inc. in 1995 [19].

1.3 Low Cost Infrared Sensors and Camera

Infrared imaging wasprimarily developed for the military applications. However, infrared imaging becomes more popular for commercial applications as the cost decreasing. Uncooled infrared detectors are good choices for low cost applications. Currently, uncooled infrared imaging is widely used for surveillance, automotive, and thermography.

Microbolometer type uncooled infrared sensors are generally lower cost thanthe cooled infrared sensors. Plus, their yields are usually higher than those of cooled detectors which should be cooled down by the use of expensive and bulky cryocoolers. On the other hand, thermopile type infrared detectors have lower responsivity compared to the pyroelectric detectors and microbolometer. Pyroelectric detectors need a chopper to obtain static images. Due to the advantages above, microbolometer type infrared detectors are generally used in the low-cost infrared imaging systems. Today, large volumes of microbolometers are produced for commercial applications.

Figure 1.8 shows the applications of the infrared imaging [39]. Military and high-end commercial applications need large number of pixels and the system cost is high. On the other hand, commercial applications like motion and temperature detection need small number of pixels and the system cost is very low compared to the military applications. At the time of writing this thesis, there is a huge opportunity for the low-cost commercial imaging applications which consist of surveillance, automotive, and thermography.

The main motivation behind this thesis is to design the first miniature infrared camera in Turkey. The designed cameras are meant to fill the gap of the low-cost commercial imaging.

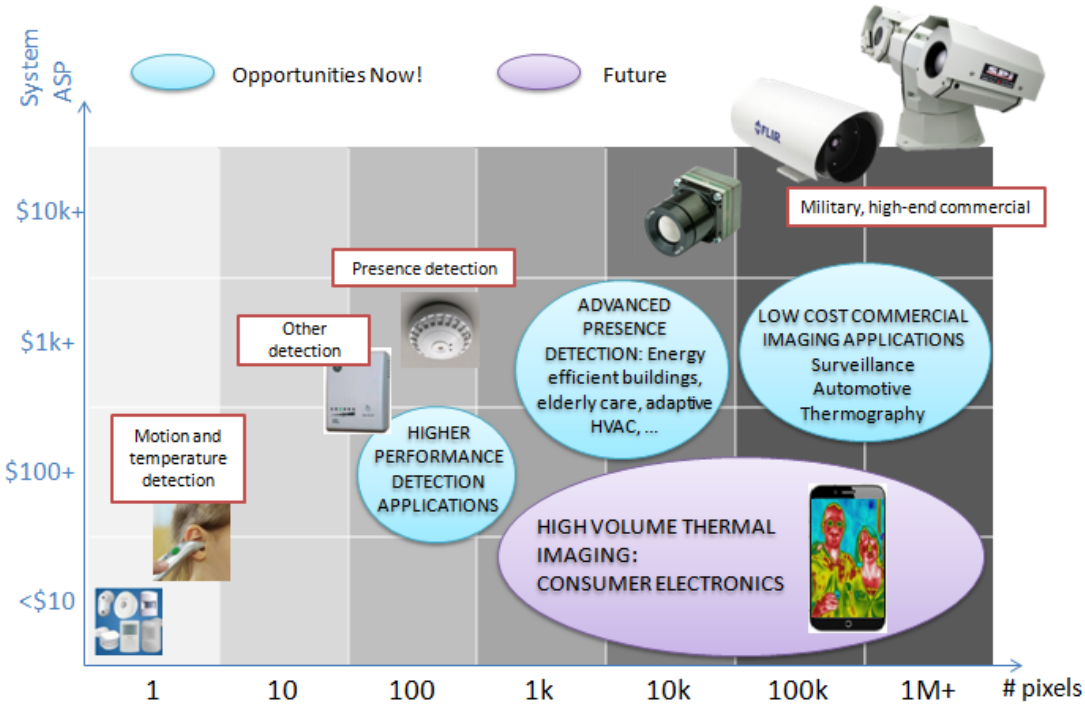


Figure 1.8: Applications of the infrared imaging [39].

Figure 1.9 shows the uncooled thermal camera business (units) [16]. It is expected that the uncooled thermal camera business will approximately reach 1,200,000 units and the commercial applications are 90% of the total applications.

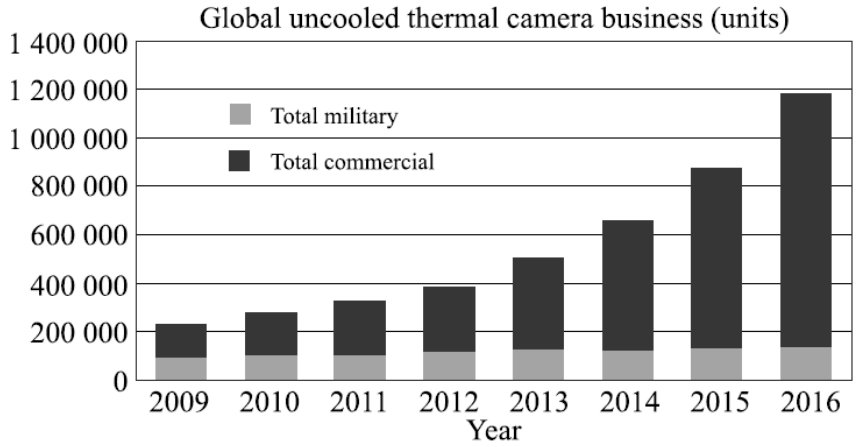


Figure 1.9: Uncooled thermal camera business (units) [16].

FLIR is one of the globally leading companies for thermal imaging infrared cameras. They released the Quark module in 2011. FLIR's Quark is the smallest and lightest fully-integrated uncooled camera core in existence. Wafer level packaged microbolometer sensors are used in this module. Figure 1.10 shows FLIR Quark uncooled core [37].



Figure 1.10: FLIR Quark uncooled core [37].

FLIR Quark uncooled core is sensitive to 7.5 to 13.5µm spectral band, andthe size of the Quark camera without lens is 2.2 × 2.2 × 1.7 mm^3. Quark is available in 336×256 and 640×512 resolution with 17µm pixel size, and power consumption of the camera is approximately 1.0 W.

1.3.1 Sensor Introduction

The camera electronics developed under the scope of this thesis are in general universal and can be easily modified for most of the uncooled thermal sensors in the literature. However, 160×120 microbolometer which is the uncooled thermal sensor developed in METU-MEMS Research and Application Center is chosen as the main product and all the camera electronics developed under the scope of this thesis are optimized for this sensor.

160×120 microbolometer described in [9, 20, 21, 22] is a diode type microbolometer. Figure 1.11shows the fabricated die photo of 160×120 uncooled thermal sensor. It has 160×120 resolution focal plane array (FPA), and it is fabricated in a standard SOI CMOS technology with 70 µm pixel pitch. The sensor is sensitive to 8-12 µm band, i.e. LWIR, of the electromagnetic spectrum. The detector is applicable for low cost applications including automotive, security and customer electronics. 160×120 microbolometer operates with 5V supply voltage and provides high swing analog output.

Each pixel of the 160×120 microbolometer has 4 serially connected diodes. Temperature of the pixel increases with the absorbed infrared radiation. Turn on temperature of the diodes change with the change in temperature.

The microbolometer operates with 2MHz clock frequency while the frame rate of it is 30fps. Power dissipation of the readout electronics of the detector is approximately 50mW. The dimensions of the chip are 14.8mm×14.5mm.

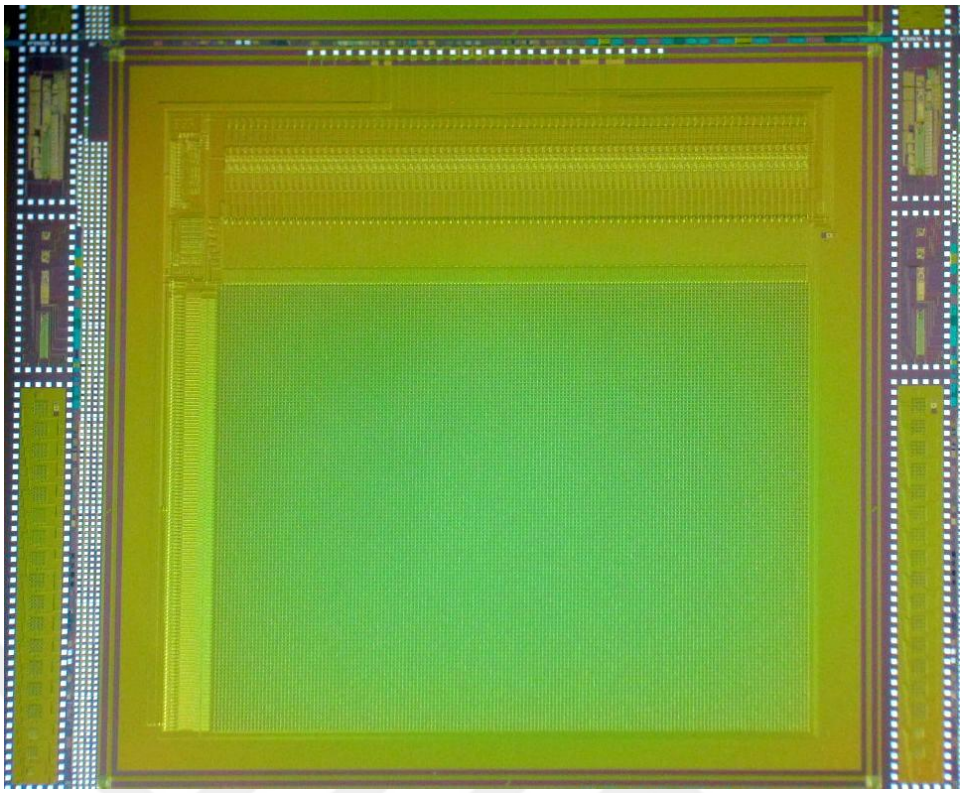


Figure 1.11: Photograph of a fabricated die of 160×120 uncooled thermal sensor.

The 160×120 uncooled thermal sensor scans the pixels in the focal plane array with rolling line methodology. In this methodology, each row of the pixels are processed in parallel so that the pixel signal is detected and amplified with very low noise preamplifier electronics and transferred to the ROIC output as a multiplexed analog signal. The sensor requires five analog biases and four digital signals. Analog bias voltages are generated by DACs while digital signals are generated by FPGA, which are all a part of the camera electronics. The sensor provides an analog output signal with 5V swing, and it can drive up to 5pF capacitive load at 30fps frame rate. An ADC is used in the camera electronics in order to convert the analog output signal of the detector to the digital domain. This digital data is used to form an image. However, because of the driving capacitive load capability of the detector output voltage, a buffer should be used to drive the ADC inputs. Table 1.1 shows the features of the 160×120 microbolometer [23].

Table 1.1: Features of the 160×120 microbolometer [23].

Features of the 160×120 Microbolometer	
Detector Size	70 µm x 70 µm
FPA Size	160 x 120
Spectral Range	8-12 µm
Mean NETD	<280 mK
Readout Integrated Circuit (ROIC) Power Dissipation	<50 mW
ROIC Output	Analog with 0-5V swing
Number of Pads	23

1.3.2 Performance Parameters of Low Cost Uncooled Microbolometer

Common performance parameters of uncooled microbolometer type thermal detectors are presented in this section. The most commonly used performance parameters are the thermal conductance (G_{th}), responsivity (R), and noise equivalent temperature difference (NETD).

Thermal conductance represents the thermal isolation level of a microbolometer. Heat loss to the ambient is caused by the support arms of microbolometer pixels. For high performance microbolometers, G_{th} value of the pixel should be minimized. The expression of the G_{th} is given as in the following equation;

$$G_{th} = \frac{\sigma_m \, x \, A}{L_{arm}} \tag{2.1}$$

where, σ_m is the thermal conductivity of the material constructing the support arm, A is the cross sectional area, and L_{arm} is the length of the support arm.

Responsivity is the ratio of the signal change in the detector to the incident power level. With higher responsivity, very small change in the absorbed infrared radiation can be read. The expression of the R is given as;

$$R = \frac{\Delta \mathrm{Vo}}{Pi} \tag{2.2}$$

where, ΔVo is output voltage change of the detector and Pi is the incident IR power on detector.

NETD is the change in the temperature of the target which generates an output signal equal to total rms noise value of the detector [19]. NETD value is very important for the low noise readout and camera electronics. The expression of NETD is shown as;

$$NETD = \frac{4F^2 V_n}{RA_D(\frac{\Delta P}{\Delta T})_{\lambda_1 - \lambda_2}} \quad (2.3)$$

where F is a coefficient related with optics, V_n is the total electrical RMS

voltage of the system, R is the responsivity of the detector, A_D is the active area of the detector, and $(\Delta P/\Delta T)_{\lambda 1\text{-}\lambda 2}$ is change of the power per unit area radiated in the λ1-λ2 spectral range.

1.4 Research Objectives and Organization of the Thesis

The main goal of this thesis is todesign and developlow cost, small form factor, low noise, and low power portable cameras, which can be powered via a USB port. Different camera electronics are designed to use the uncooled microbolometer type infrared detectors for different purposes.

The main objectives of the thesis are listed below:

1. Design and development of the portable camera systems for uncooled infrared sensor. The designed portable camera systems provide a high performance, low cost, low noise, and a small form factor system.
2. Design of the digital interface and USB communicationboard. Thisboard is designed to minimize the cost of the camera system. The camera system is powered through a USB cable with the newly designed board.
3. Design and development of the miniature uncooled infrared camera. Ultra small size, low noise, low power camera systems are produced with these designs.
4. Design of the miniature version of the digital interface and USB communicationboards. Miniature camera system can be used with the miniature version of the digital interface and USB communication board, and USB powered system is achieved.

The thesis organization is as follows:

Chapter 2 gives the information about the designed camera electronics. Both the portable and the miniature camera electronics are explained in detail and the board layers of each board in the camera are presented. Chapter 3 describes the implementation of the camera systems. Implementation includes mechanical design of the camera, housing, and optics. Chapter 4 shows the test results of the designed camera electronics. Noise, power consumption, and size of the designed camera electronics are presented in this chapter.

CHAPTER 2

CAMERA DESIGN FOR LOW COST UNCOOLED MICROBOLOMERS

2.1 Introduction

The concept of this thesis focuses on the development of ultra-portable, small volume, high performance, and low cost camera electronics proper for uncooled thermal sensors. Although the camera electronics developed under the scope of this thesis are universal and can be used with many different sensors after minor modifications, the uncooled thermal camera core developed at METU-MEMS Research and Application Center of Middle East Technical University is used as the primary sensor for the most of the electronics.

The first milestone of this thesis is the design of the first *portable camera electronics* for 160 × 120 microbolometer. The portable camera electronics developed under the scope of this thesis mainly focuses on portability and functionality.

The miniature camera electronics for 160 × 120 microbolometer is developed aiming maximum portability with the experience gained during the design and verification of the portable camera electronics. The miniature camera covers a volume of only 29.8cm^3 and can be operated using USB power of a computer. Chapter 2.6 gives detailed information on the miniature camera electronics. The designed miniature camera electronics provides high performance imaging with very low power dissipation and volume requirement.

Moreover, board layouts are shown in Section 2.7. The camera performance is directly affected from the grounding of the boards. Therefore, some of the layers of the camera boards are shown in Section 2.7.1. Also, ground and power distribution of each camera is explained in Section 2.7.2 in detail.

2.2 Design Guidelines for High PerformanceCamera Electronics

The uncooled thermal sensor, the camera electronics, and the optical accessories form a thermal imaging system. The ultimate performance of the imaging system is determined by all the parts of the system. In order to achieve maximum performance, all parts of the system should be optimized. Thus, even a very high performance sensor may yield poor performance with bad camera electronics.

Camera electronics performance is affected by many different concepts like on-board noise sources; crosstalk between signals, grounding, power distribution, ground bounce, board to board connections, USB powered components, and analog signal flow. The rest of this section will summarize these concepts.

2.2.1 Crosstalk

Crosstalk is a transfer of energy between two parallel signals that are placed closely, and it affects the system performance. The transferred energy causes an undesired coupling between the signals. Therefore, different signals should be prevented from interfacing in order to minimize crosstalk. Analog and digital signals should be separated, also both high level and low level analog signals should be separated each other. Ground planes are also important parameters to minimize the crosstalk [24, 25].

2.2.2 Power and Ground Routings

Grounding is one of the most important parameters in order to design high performance camera. Ground planes are used to decrease the ground impedance, and it covers a huge section which is a copper area in the board. These planes have low resistance because of the large metal area in the PCB. Ground pins of all circuits should be connected directly to the low impedance ground plane. Figure 2.1shows the middle layer of the power board of the miniature camera.

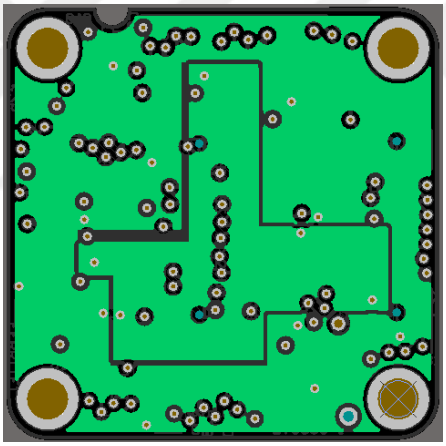


Figure 2.1: The middle layer of the power board of the miniature camera.

Usually there are more than one power signal in complex systems and these power signals may be separated from each other in order to decrease electrical cross talk. In such cases the star connection technique is usually used. Star point grounding technique is used to isolate grounds of the components. This technique avoids the interfacing of the ground currents between the components [26]. Each component connects to a system ground directly at a start ground point. Figure 2.2 shows the star grounding scheme.

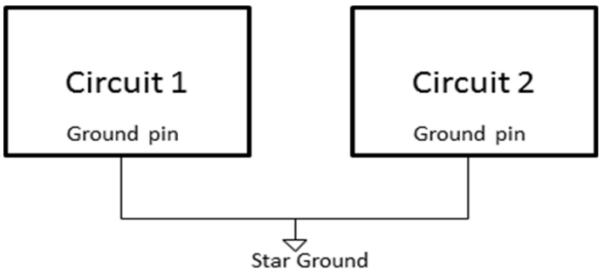


Figure 2.2: Star grounding scheme.

Grounding of the mixed signal ICs are also very important. ADC and DACs are used in the camera electronics will be discussed in Section 2.5 and Section2.6. Figure 2.3 shows grounding of mixed signal circuits. ADCs and DACs are the examples of mixed signal circuits and they have both analog and digital circuits in them. The grounds of the analog and digital blocks inside the circuit should be separated to avoid the coupling between analog and digital signals.

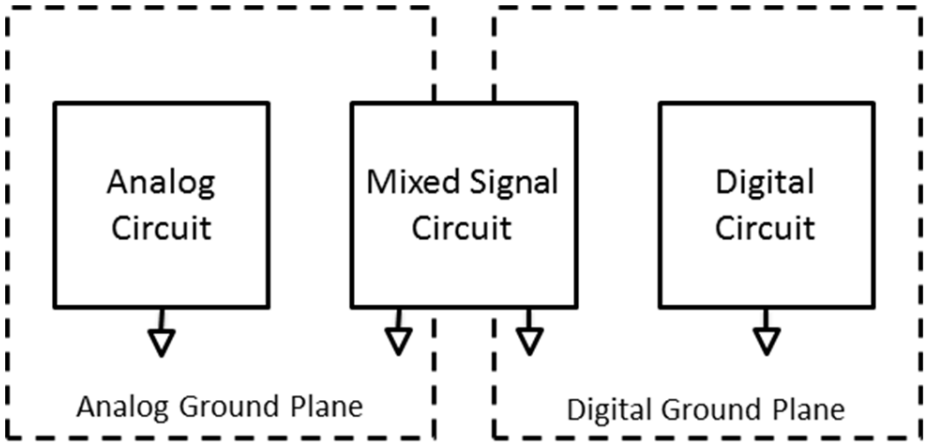


Figure 2.3: Grounding of mixed signal circuits.

Power distribution is as important as the grounding in order to have a high performance camera. Power planes and power bus networks are generally used to distribute the power of the components [27]. Because power planes cover huge areas, they are generally used in the multilayer PCBs; on the other hand, power busses are generally used in the one layer PCBs because they consist of multi metal traces that carry power. Power busses have significant DC resistances, and it is the main drawback of them [27]. In the designed camera electronics, power planes are used to distribute the power from the source to the ICs. Power distribution of each designed cameras is explained in Section 2.7.2.

2.2.3 Supply Decoupling

Supply decoupling is another important concept regarding a high performance camera. Decoupling capacitors are used to shunt high frequency noise away from the power signals of the components [25]. Ceramic decoupling capacitors with low impedance, low inductance, and low series resistance are used for decoupling.

2.2.4 Ground Bounce

Ground bounce is the change of the ground voltage with respect to the main board ground voltage. It occurs when there is a simultaneously current change on the power line [28]. A voltage is generated between the device ground and board ground because of the inductance of the electrical lines carrying the power signals. Amplitude of the ground bounce depends on many different parameters; number of activities of digital circuits, capacitive charging of the analog blocks, etc. When the amplitude of the ground bounce is relatively high, the performance of the board is affected from this ground bounce.

In the designed camera, the analog output of the detector is converted into the digital domain using ADCs. Figure 2.4 shows the representative view of grounding of the ROIC and ADC in the designed camera electronics. Because of the non-zero resistance and inductance of the electrical lines carrying the power signals, a certain impedance appears between the local grounds of the ADC and ROIC. This inductance creates ground bounce and instant change in the ground voltage during activities of the components. A voltage reference generator is embedded into the circuit as shown in the Figure 2.2. In order to minimize the effect of the ground voltage change. Basically, ADC converts IN+ voltage with respect to IN- which is generated by a reference voltage generator referring the local ground of the ROIC. By the use of this method, the effect of instant ground voltage change is eliminated.

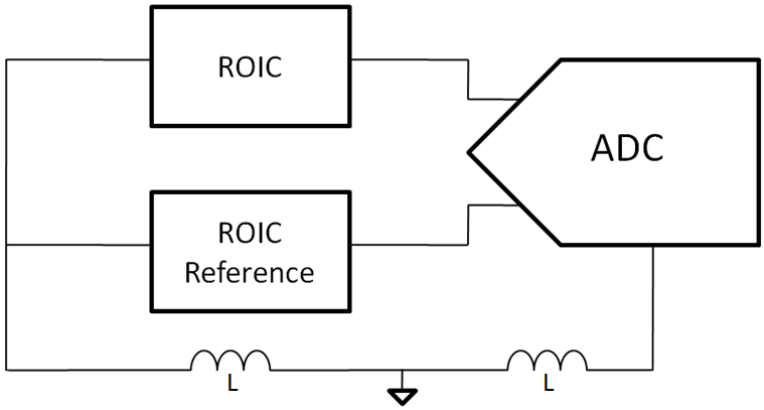


Figure 2.4: Representative view of grounding of the ROIC and ADC in the designed camera electronics.

2.2.5 Board to Board Connections

In the scope of the thesis, two different camera electronics are designed, and they have a stacked structure. Connectors are used to stack the camera electronicsboard to form a camera.

Connectors have mutual inductance, series inductance,and parasitic capacitance. Mutual inductance causes crosstalk between the signals. Noise is introduced because of the magnetic fields caused by the overlapping return paths. Series inductance is resulted from mostly the pin length of the connectors, and the pin layouts of the connector determine the electromagnetic interference [29].Series inductance can be minimized by using more than one pin for a signal so that the inductance decreases by parallel combinations. Parasitic capacitance slows the signal propagation [30]. Therefore, connectors with low parasitic capacitance should be preferred.

2.2.6 USB Powered Devices

The Universal Serial Bus (USB) powered devices are powered up through the USB ports. USB powered systems have many advantages. The most important advantage of the USB powered system for the applications that are used in the scope of the thesis is that the USB powered systems do not require power supply. The host equipment provides 5V supply from the power supply of the computer hub, and it can draw up to 500µA quiescent current. Therefore, with the USB powered system, the infrared camera system consists of only the computer and the portable camera. In addition, USB powered system is easy to connect system with only one cable that consists of power, ground, and two data signals. It can support different device speeds up to 480 Megabit/sec [31].

In this thesis, both external DC supply and USB powered systems are used in the designed camera electronics. In the supply powered systems, 6V supply voltage is used to have 5V analog and digital detector supply voltages. Supply voltage should be applied higher than 5Vto have a regulator output of 5V because of the dropout voltage of the regulator,. However, in the USB powered systems, the low dropout regulators cannot be used. Therefore, a switch capacitor voltage converter is used to obtain 5V.

The most important fact of using the USB power is that, the USB power signals are usually more glitchy compared to the low noise DC supplies. Therefore the USB power should be carefully engineered in order to achieve low noise and high performance systems.

2.2.7 Analog Signal Flow

In the analog signal block of the camera electronics, the analog output signal of the detector is buffered and the buffered signal is applied to the input of an ADC. Figure 2.5 shows the block diagram of the analog signal block. The analog output of the signal is buffered because of the analog output capacitance drive capability, and the signal is converted to the digital domain to obtain an infrared image. Using a buffer between the ROIC and the ADC also helps the signal settling and decreases the kick-off effects usually appearing on the ROIC output because of the fast transitions in the ADC.

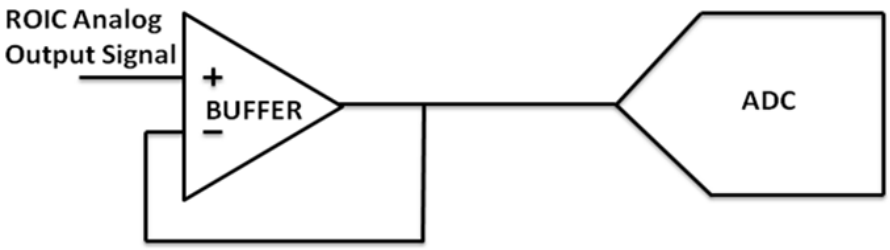
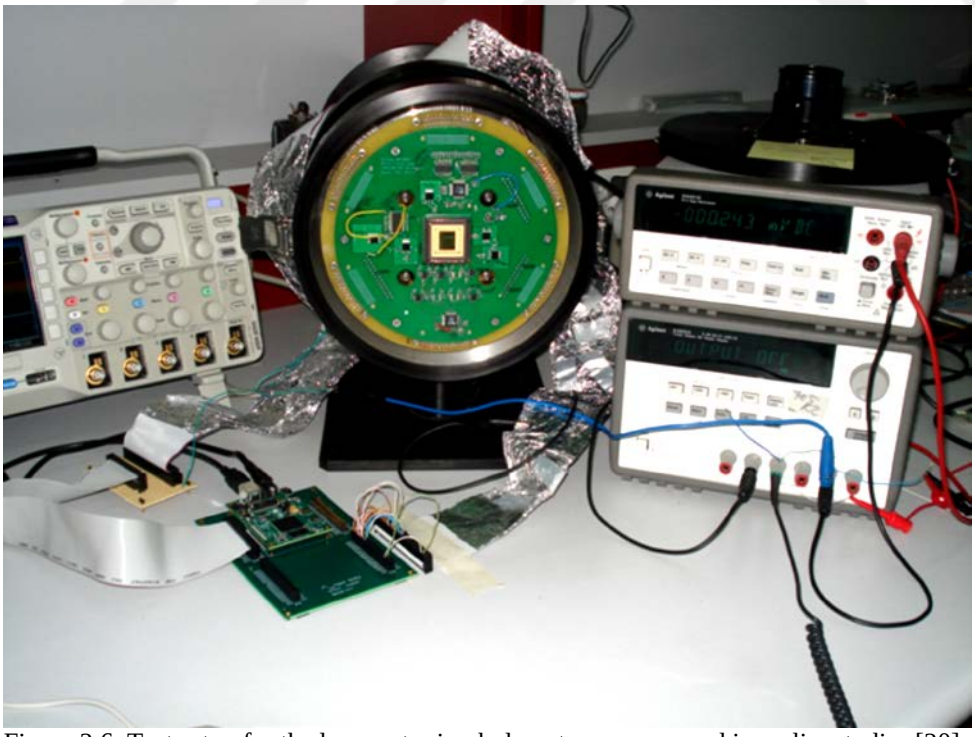


Figure 2.5: Block diagram of the analog signal block.

2.3 Previous Works on Camera Design in METU

This section summarizes the previous works on camera design at METU-MEMS Research and Applications Center. In the previous works, large form factor vacuum DEWARs were used and camera electronics were developed for these DEWARs by the METU-MEMS group members. Figure 2.6 shows the test setup for the low cost microbolometer camera used in earlier studies [20]. The camera is composed of a dewar board, a routing board, and a digital interfaceboard as shown in Figure 2.6. In addition, Figure 2.7 shows an image taken with 160×120 microbolometer and dewar setup [20].


Figure 2.6: Test setup for the low cost microbolometer camera used in earlier studies [20].

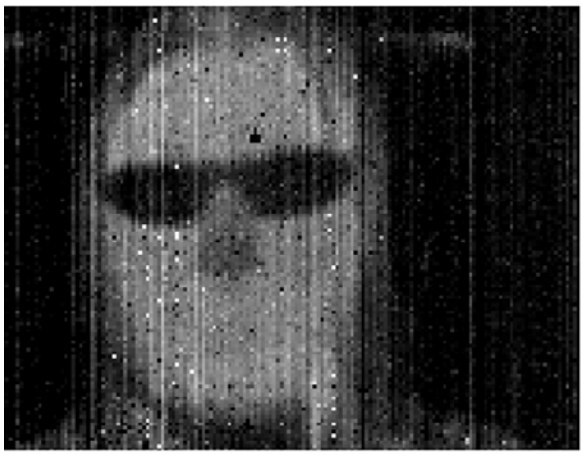


Figure 2.7: An image taken with 160×120 microbolometer and dewar setup [20].

As the prior work of this thesis study, a design process of a more compact hand-held camera is started and the initial pseudo-compact camera electronics are realized by the writer of this thesis. Since the resulting camera is not really portable, this study is not included in the scope of this thesis. Figure 2.8 shows the photograph of the resulting hand-held camera of this prior study. The electronic design of the handheld camera has similarities with the previous camera electronics used in the dewar. The camera consists of five different boards: sensor interface board, analog board, power board, digital level translator board, and a commercial digital interface board. These boards are stacked with connectors, one on top of another, and form a camera. The boards of the camera cover an area of 8.9×5.3 cm^2.

Although this camera design is not included in the scope of this thesis, it is the first minor step towards the miniature camera electronics.

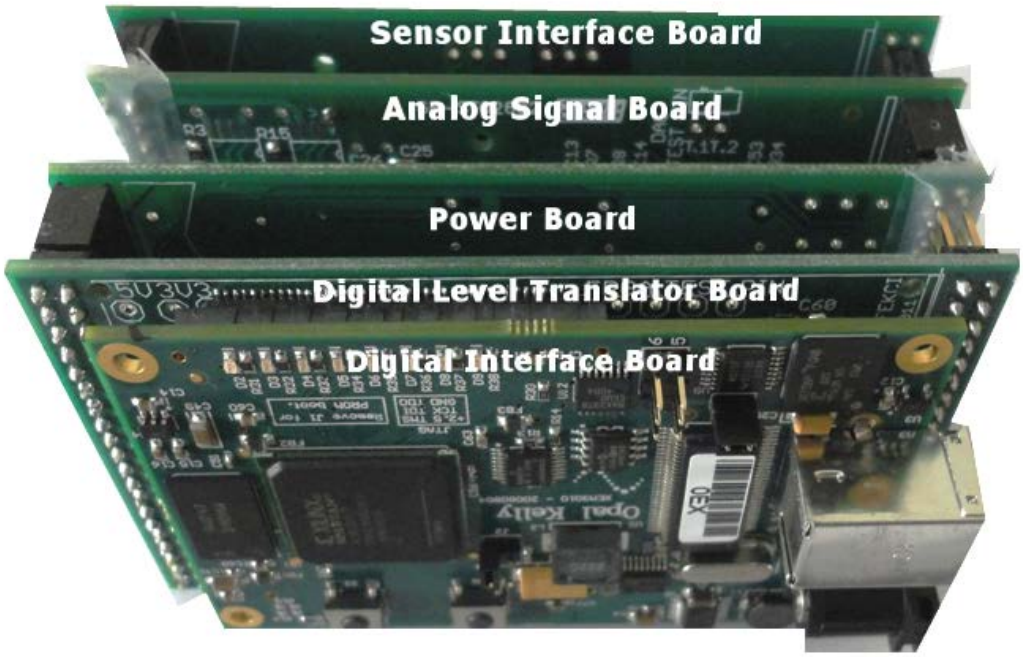


Figure 2.8: Photograph of the handheld camera.

2.4 Design Cycle of the Portable and Miniature Camera Development

The motivation behind this thesis is to design and develop the small form factor, low cost, and low noise camera proper for low-cost microbolometer type infrared detectors. Figure 2.9 shows the design cycle of the camera electronics. Firstly, the schematic of the camera electronics is designed. After that, components of the schematics are simulated. Simulations of the components are necessary to minimize the risks of the design. If the simulation file of the components that are used in the camera does not exist, the camera electronics is designed with respect to the datasheet. In addition, components that are recommended in the datasheet are used in the design to minimize the risks. Then, the layout of the boards is designed. At the end, the board is fabricated after the generation of the Gerber files of the boards.

Main bottlenecks of the camera design are to achieve low noise and low cost camera electronics within a small form factor. The mechanical design of the camera is also important in order to have a small, compact and hand-held camera.

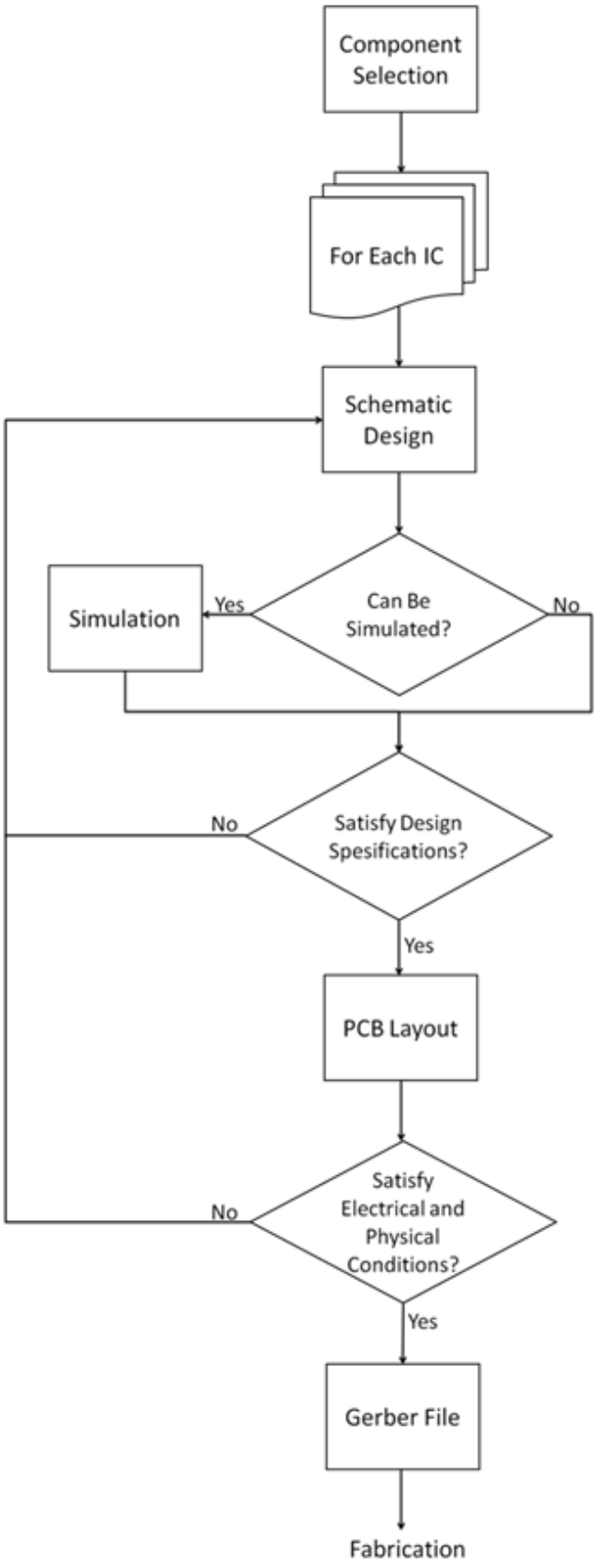


Figure 2.9: Design cycle of the camera electronics.

2.5 Portable Camera Electronics

The portable camera electronics is designed and developed in order to have a portable and compact camera. Figure 2.10 shows the block diagram of the portable camera which consists of sensor interface board, camera electronics board, and digital interface and USB communication board. Low noise, small package, and low cost components are chosen in order to design the low-cost and portable infrared camera. The infrared sensor is soldered on top of the sensor interface card which is mainly a connector card routing the electrical signals to the next electronic cards. The noise rejecting bypass capacitances are also placed on the sensor interface card. The camera electronics board does most of the job, which can be summarized as generating the required power signals, converting the analog output of the sensor chip to digital, generating the required analog bias voltages, and making the connection between the digital interface board and the sensor. The digital interface and USB communication board generates the digital timing signals for the sensor and the components on the camera electronics board, and links the camera electronics with the computer via the USB interface. This board uses a low cost, small size and low power FPGA together with a USB interface chipset. The details of these cards will be summarized in the next sections.

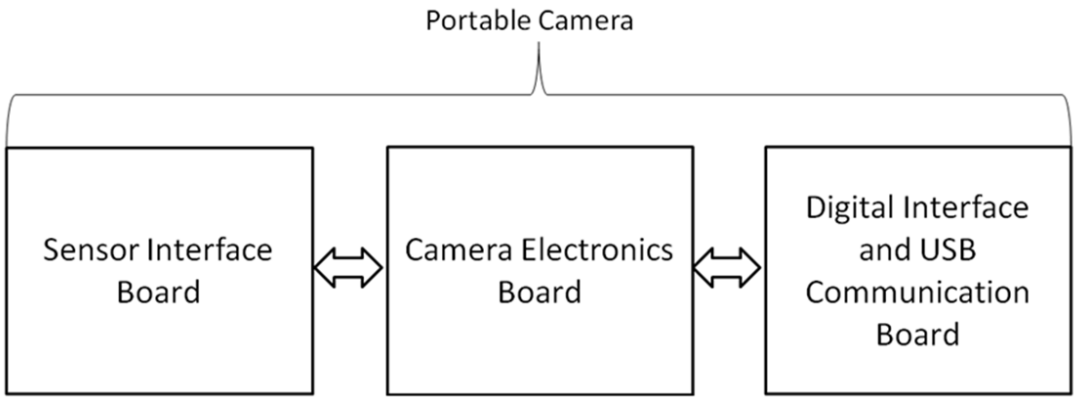


Figure 2.10: Block diagram of the portable camera.

2.5.1 Sensor Interface Board

The 160x120 microbolometer is placed on the sensor interface board of the portable camera. The board covers an area of 3×3 cm^2.Sensor and required bypass capacitors occupies the sensor interface board. Different sensor interface boards can be used with same camera electronics board.

Each infrared sensor chip under test is soldered on top of a sensor interface board, so that one camera electronics board to be described in the next section can be used for more than one sensor interface boards. By this approach, many infrared sensor chips can be tested with a single camera electronics board.

2.5.2 Camera Electronics Board

The camera electronics board is the second board of the portable camera. It covers an area of 5×7.5 cm^2. Figure 2.11 shows the block diagram of the camera electronics board of the portable camera. The board is composed of the power block, analog signal block, and digital level translator block.

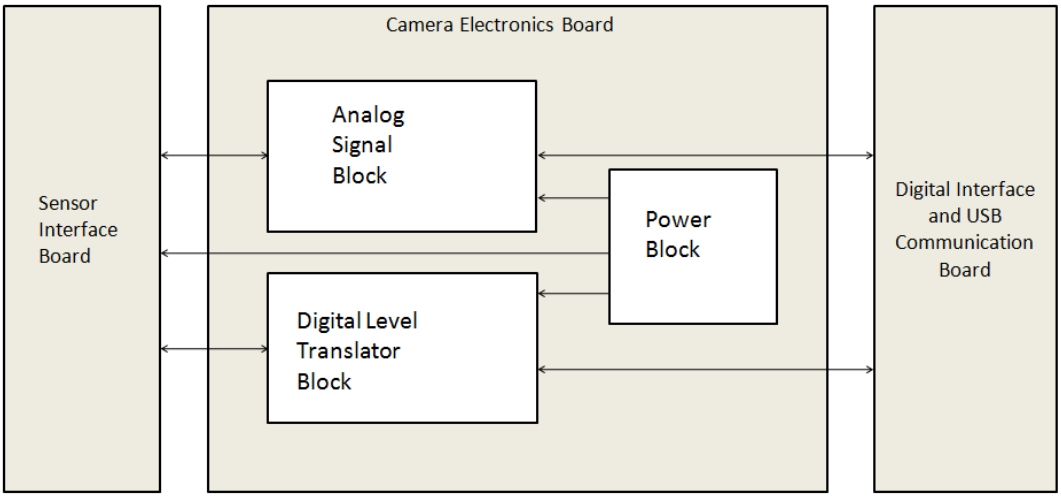


Figure 2.11: Block diagram of the camera electronics board of the portable camera.

Figure 2.12 shows the power block diagram of the camera electronics board. The power block of the camera electronics board consists of seven regulators. LT1762 series regulators are used in the portable camera, and they are micro power, low noise, and low dropout regulators. They have a maximum dropout voltage of 270mV with a 150mA maximum output current. The supply power of the camera is applied to the camera electronics board from desktop a power supply. 6V is applied from the power supply to obtain 5V and 3.3V regulator output voltages. The 160x120 microbolometer needs 5V digital, and 5V analog supply voltage. Two of the regulators are used to feed digital and analog sensor supply voltages. The regulator fed the analog sensor voltage, also feed DACs. Two of the regulators are used for the digital level translator because it needs both 5V and 3.3V supply voltage. One 5V regulator and one 3V regulator are used to feed the buffer and ADC, respectively.

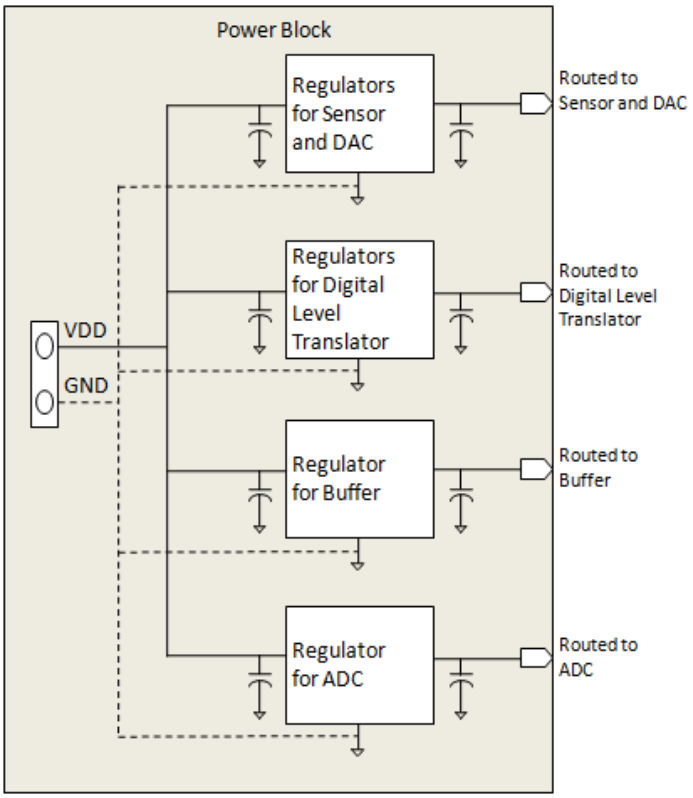


Figure 2.12: Power block diagram of the camera electronics board.

Figure 2.13 shows the digital level translator block diagram of the camera electronics board. The 160×120 microbolometer operates with the 5V digital supply. Therefore, a digital level translator circuit should be used to solve the 3.3V and 5V interface problems between the digital I/Os of 3.3V FPGA and 5V sensor. A digital level translator, namely MAX3002, is used for the 3.3V and 5V interface problems. It has 8 outputs, and it is a bidirectional data translator.It is used to shift both 3.3V signals to 5V as well as 5V signal to 3.3V. Besides it allows data translation in either direction on any single line data.

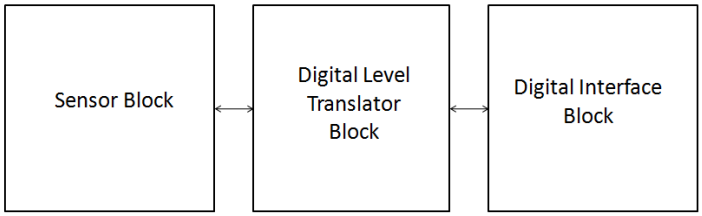


Figure 2.13: Digital level translator block diagram of the camera electronics board.

Figure 2.14 shows the analog signal block of the portable camera electronics. The analog signal block is composed of a DAC, a video buffer, a video opamp, and an ADC. One channel analog output signal of the sensor and reference signal of the analog output provided by LTC2640 are buffered using LT1807 dual buffer. Thisdual video buffer is a rail to rail input and output, low distortion, low noise precision opamp. The analog output signal of the detector is buffered in order to drive an ADC. The video buffer has 60ns settling time, and it has 20Ω output impedance at 100 MHz. These properties make this buffer a good choice for driving A/D converters.

Buffered analog output signal of the sensor has an approximately 0V to 5V swing. An analog input of the ADC, namely LTC1403, operates with 0V to 2.5V differential swing. A video opamp, ADA4853 - 3, is used to have 0V to 2.5V analog output swing. This video opamp is a triple, low power, and rail to rail output video opamp, and it is used to divide the buffered signals by two.

The analog output signal is converted to digital domain to form an image. The conversion is done with an ADC. In the portable camera LTC1403 ADCis used to achieve low power, low cost, and small form factor camera electronics. It is a 14 bit, 2.8Msps serial output ADC with differential inputs. It needs a single 3V supply, and it has typical 12mW power dissipation in active mode.

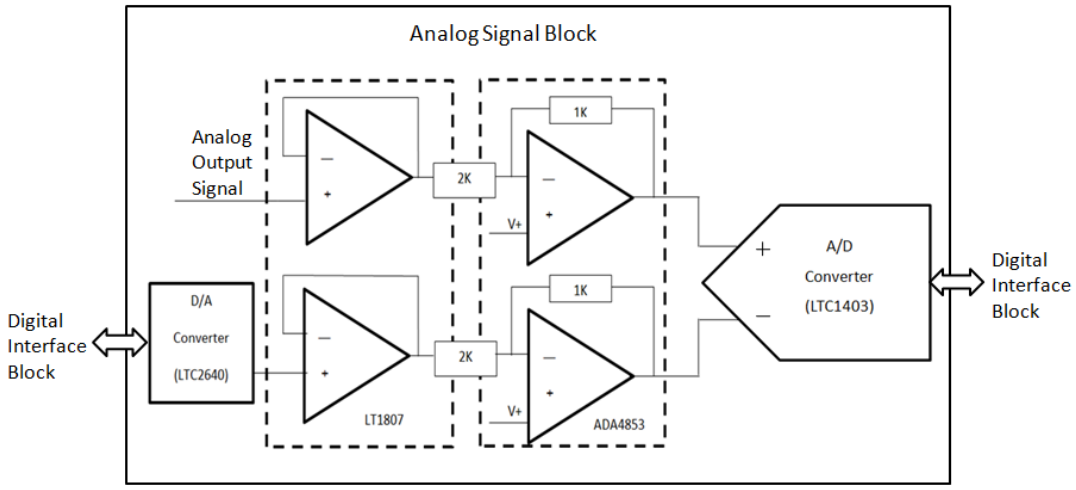


Figure 2.14: Analog signal block of the portable camera electronics.

In the portable camera electronics, two more DACs, namely AD7399, are used to provide the analog bias voltages of the detector. It is a serial input, quad, 10 bit DAC, directly programmed by FPGA. There are two DACs used in the portable camera because detector needs 7 analog bias voltages.

2.5.3 Digital Interface and USB Communication Board

A digital interface and USB communication board is designed in the scope of this thesis in order to replace the commercial digital interface boards used before this newly designed board. The cost of this digital interface and USB communication board is much lower than the previously used commercial FPGA board. Thus, the design of a custom digital interface and USB communication board was a must in order to obtain a low cost camera system.

Figure 2.15 shows the block diagram of the digital interface and USB communication board. The board consists of the power block, digital interface block, and USB communication block.

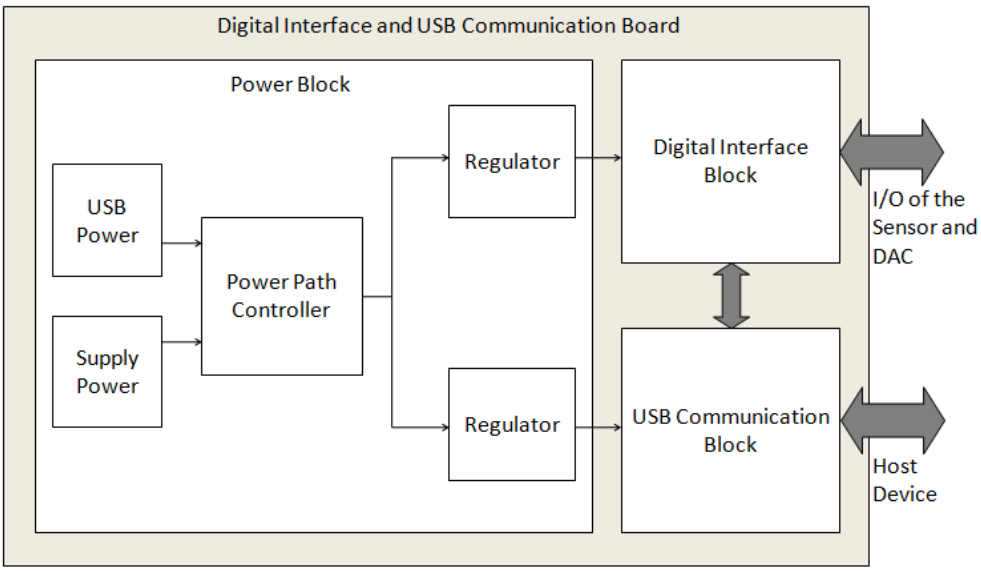


Figure 2.15: Block diagram of the digital interface and USB communication board.

The digital interface and USB communication board can be powered through a small power connector or a USB interface. If both of the connectors are plugged in, the board will be powered through the power connector. If the power connector is unplugged, the board will be powered through USB. The supply voltage of the board is 5V supply from both of the inputs. The power options are controlled with a low loss power path controller IC,namely LTC4412. It is used with P-channel MOSFET to permit efficient OR'ing of different power sources with typically 20mV voltage drop. Also, there are two LT3080 regulators used for supply voltages of the digital interface unit. They are adjustable, low dropout regulators and used because of the high output current property of 1.1A. It has maximum 300mV dropout voltage with a 1.1A output current. Digital interface IC needs both 3.3V and 1.5V supply voltages that are provided by these regulators. Moreover, USB communication block needs a 3.3V external power source. Therefore, one more regulator is used in the board for this block. ADP124 is a low quiescent current and

CMOS linear regulator, and it is used to generate the required 3.3V supply source for the USB communication block. It has 500 mA output current and an adjustable output voltage.

The digital interface block is composed of an FPGA, an oscillator,a reset circuit, and a programming header. ACTEL IGLOO nano series AGLN50V5-VQG250 FPGA is used in the digital interface and USB communication board. It is a very low power and small form factor FPGA and it has up to 250,000 system gates and 250 MHz system performance. The FPGA needs 20 MHz clock oscillator. Very small size TXC series 20 MHz crystal oscillator is used in the digital interface block. It needs 3.3V supply voltage, and it is provided by one of the LT3080 regulators described in the power block of the board [19]. In addition, a push button reset switch with a microprocessor reset circuit, TS809CXD,is provided for reset option. It is used to assert a reset signal when supply voltage declines below a threshold value [32]. There is a push button switch with a small size in the board. Moreover, there is a 12-pin male programming header placed to the board. The FPGA can be programmed through the programming header with an external low cost programming stick. The programming header is needed only during the programming of the FPGA.

Furthermore, a USB 2.0 high speed to UART/FIFO IC, namely FT2232H, is used for USB protocol engine. USB to UART interface provides a standard UART connection with the digital interface block. FT2232H consists of +1.8V low dropout integrated regulator. The regulator generates 1.8V for the core and the USB transceiver cell. There is an integrated EEPROM interface in the USB communication block for a USB to dual asynchronous serial port device. In addition to integrated EEPROM, one more external EEPROM is used for each of the chip's channels to have an independent configuration. Table 2.1shows the technical specifications of the portable camera.

Table 2.1: Technical specifications of the portable camera.

Portable Camera	
Number of PCBs	3
Physical Dimension without Housing	$7.5\times5\times2cm^3$
Physical Dimension with Housing	$7.9\times5.4\times2.2cm^3$
Sensor	160 × 120 microbolometer
Power Signal	6 V
Regulators	7 LT1762 low dropout regulators.
DACs	2 AD7399 10 bit, quad DACs. 1 LTC2640 10 bit DAC.
ADC	1 LTC1403 with series digital output and 2.8 MSPS conversion rate
Digital Level Translator	1 MAX3002 with 8 outputs.
Video Transfer	Via USB protocol
Power Dissipation	0.55 W

2.6 Miniature Camera Electronics

The main motivation about the miniature camera development is to carry the portable camera concept one step further and make it possible to even use thermal camera cores with highly portable system such as cellular phones or tablets. Figure 2.16 shows the block diagram of the miniature camera. The miniature camera consists of sensor interface and analog signal board, power board, digital interface board, and USB interface board. The miniature camera boards cover an area of $2.9\times2.9\ cm^2$.The sensor interface and analog signal board consists of the infrared sensor, that is soldered on top of the board, the digital level translator block, and the analog signal block. The power board generates the required power signals and the analog bias voltages of the sensor. The digital interface board generates the digital timing signals for the sensor, DACs and ADC. The USB communication board links the camera with the computer via the USB interface. The details of each board will be explained in the next sections.

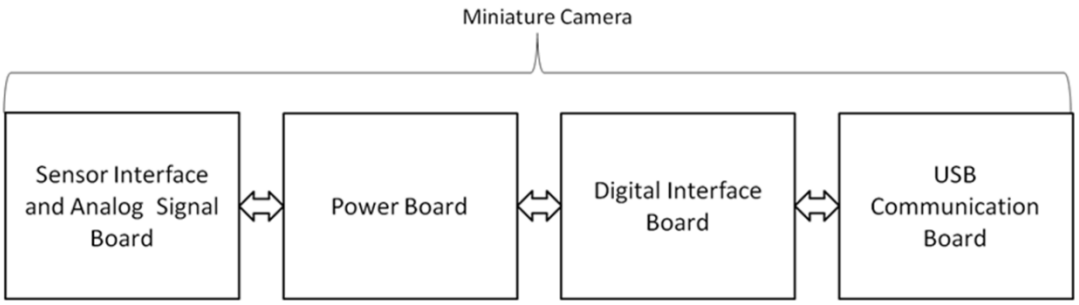


Figure 2.16: Block diagram of the miniature camera.

2.6.1 Miniature Sensor Interface Board

Miniature sensor interface board is designed to have a high performance and low noise miniature camera core. Figure 2.17 shows the block diagram of the miniature sensor interface board. This board is mainly consists of the sensor, analog signal chain block, and digital level translator block. The 160×120 microbolometer is used in this camera.the board is composed of two voltage references to provide reference signal of ADC and common mode signal of the single ended to differential converter, a single ended to differential converter,an ADC, and a digital level translator are placed to the sensor interface board. Figure 2.18 shows the analog signal block of the miniature camera. The critical analog blocks such as the bandgrap references and ADC is placed on this board very close to the sensor chip in order to minimize the ground looping and bouncing problems, which is very crucial for high performance systems.

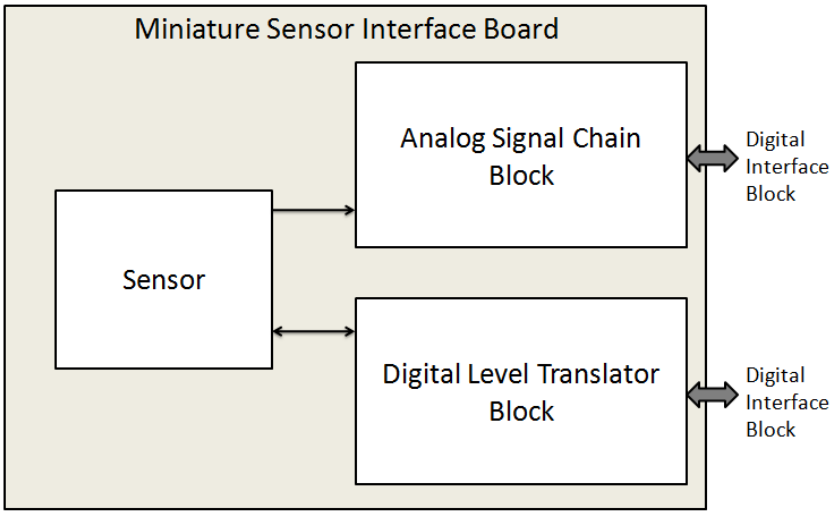


Figure 2.17: Block diagram of the miniature sensor interface board.

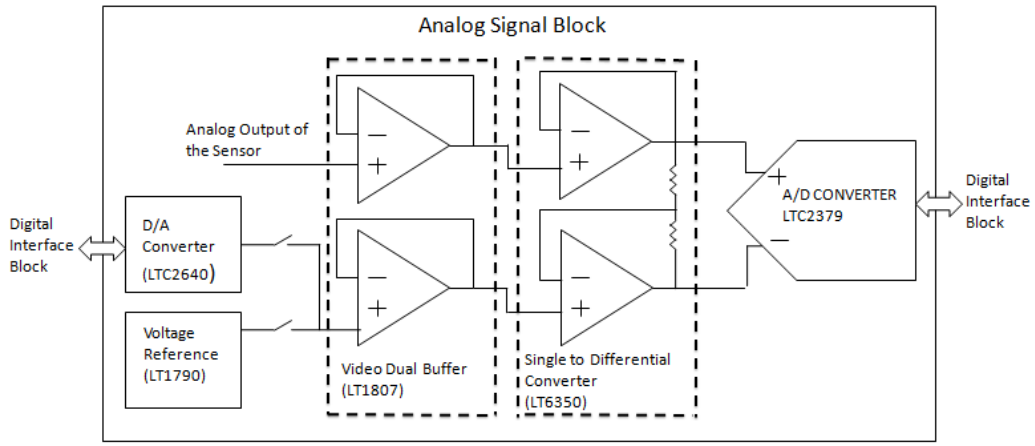


Figure 2.18: Analog signal block of the miniature camera.

The analog signal block of the camera is composed of a voltage reference, a DAC, a video buffer, a single ended to differential converter, and an ADC. The reference signal of the analog output signal of the sensor is provided by either a DAC or a low noise voltage reference. The same dual buffer is used in the miniature camera as the portable camera. However, reference voltage and the dual video buffer are not used in the default configuration since the single to differential converter buffers the analog signal of the detector.

A low noise, low power, 18 bit, and 1.6Msps SAR ADC, namely LTC2379, is used in the miniature camera. It has 18mW power dissipation and a fully differential input range between –VREF to +VREF with reference voltage ranging from 2.5V to 5.1V. In this design, VREF is applied from 5V voltage reference IC. The input range of the ADC is 0V to VREF. Therefore, there is no need to use voltage divider circuit as portable camera electronics when 5V reference is used. The ADC needs 2.5V power supply and 3.3V I/O interface digital power. There are four digital I/O pins in the ADC, namely convert input to initiate conversion, busy indicator, serial data clock input, and serial data output. These four digital I/Os can directly communicate with the FPGA without any need of digital level translator because of the 3.3V I/O interface digital power. The ADC digitizes the full scale voltage into 2^{18} levels, so the size of 1 LSB is 38µV if VREF is 5V. A buffer should be used before the ADC to provide low output impedance and isolation between the signal sources. It also avoids the current spike that the ADC inputs draw. A single ended to differential converter, namely LT6350, is used in the camera electronics for both buffering the analog output of the detector and producing a differential signals at the inputs of the ADC. LT6350 is a rail to rail input and output, low noise single ended to differential converter and an ADC driver. It is used to convert single ended input signal, which is analog output signal of the detector with approximately 0V to 5V range, to differential signal. There are two opamp topology used in the LT6350. The first amplifier is used as a unity gain buffer, which results in buffering the single ended analog output signal. The second amplifier is a unity gain inverter with externally applied common mode voltage level. The common mode voltage is applied from the reference signal of the ADC. The 5V reference signal is divided with a voltage divider and applied to common mode signal of the single ended to differential converter.

Various simulations are carried out in order to verify the operation of the single-to-differential converter. As an example, Figure 2.19 shows the results of a spice simulation which shows the operation and common mode rejection of the converter. During the normal operation the single-to-differential converter generates a differential signal by using the single-ended analog input and common mode voltage. The single-ended analog input is converted to differential by subtraction

of the signal around the common mode voltage. In case of a common noise on the analog input and the common mode voltage, the single-to-differential converter is expected to reject this common mode noise and generate a common-mode noise free differential output. This property is verified in the simulations shown in Figure 2.19. Common mode signal of the converter (v_{cm}), indicated by pink, is applied from 2.5V LT1790 voltage reference. The sensor output, which is the analog input in this simulation, is represented by a square wave with 3 V swing and 50 kHz frequency. A common sinusoidal signal, which corresponds to a noise or difference between the ground signals, is also added to common mode signal and analog input signal. The analog output signal of the detector (v_{in}) and the first output of the converter (out1), indicated by green and blue, respectively, are exactly same. The second output of the converter (out2) is indicated by red. "out1" and "out2" signals are the input signals of the ADC (LTC2379), and they are fully differential with respect to "v_{cm}" as shown in Figure 2.19. The simulation result shows that the output signals of the single to differential converter are fully differential with respect to the common mode signal that is applied by a voltage reference. The common sinusoidal noise of the analog input and common mode signal is successfully rejected and a common-mode noise free differential output is obtained.

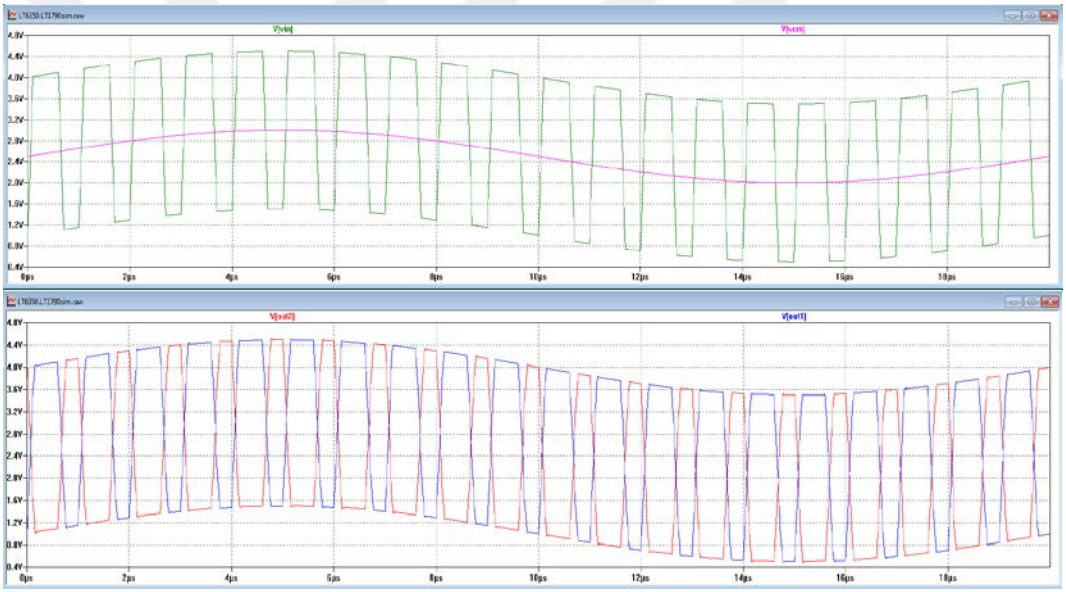


Figure 2.19:Spice simulation result of the LT6350 single ended to differential converter.Common mode signal of the converter (v_{cm}), analog output signal of the detector (v_{in}), the first output of the converter (out1), the second output of the converter (out2) indicated by pink, green blue, and red, respectively. "out1" and "out2" signals are the input signals of the ADC (LTC2379), and they are fully differential with respect to "vcm".

The digital level translator block is same with the Figure 2.13. In the miniature camera electronics, the same digital level translator is used as the portable camera in order to solve 3V/5V interface problems. Digital I/Os of the sensor signals are converted both from 5V to 3.3V and 3.3V to 5V with using the digital level translator.

2.6.2 Miniature Power Board

Figure 2.20 shows the block diagram of the power boards of the miniature camera. The miniature camera is powered through a power connector or a USB. Two different miniature power boards are designed. 6V supply voltage through power connector or 5V DC USB voltage is applied.

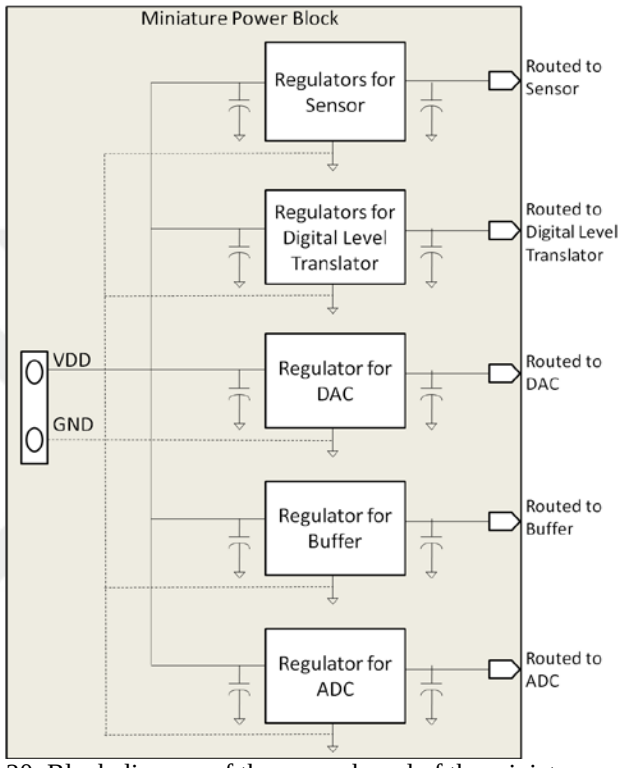


Figure 2.20: Block diagram of the power board of the miniature camera.

One of the miniature power boards is optimized for the USB power. 5V DC USB supply voltage is used for the sensor and some of the components in the camera electronics. Therefore, it is impossible to use LT1762 regulator to maintain a constant 5V voltage level because of its low dropout property. LT1762 has maximum 270mV dropout voltage with 150mA output current, and it is a critical dropout voltage level for the 160×120 microbolometer sensor. Therefore, a new component, TPS60241, is used to apply 5V regulated voltage level with USB powered system in this board. TPS60241 is a zero ripple switched capacitor voltage converter. The input voltage of it is between 2.7V and 5.5V for 5V output voltage. Output current of it is 25 mA, which is very low with respect to LT1762, but it is more than enough for this system.

The difference between the power block of the portable and miniature camera is only TPS60241 regulator. The five 5V low dropout regulators used to apply 5V supply voltages to the components in the portable camera are changed with 5V TPS60241. Therefore, in the miniature camera five

TPS60241 voltage converters are used. Two of the converters are for the digital and analog 5V supply voltage of the sensor while one of them is for DACs supply voltage. 5V digital level translator supply voltage is applied from one of the converter, and the last one is for the buffer supply voltages. In this board, power can be applied both from the power board or USB communication board.

18 bit LTC2379 ADC is used in the miniature camera. Two of the LT1762 low dropout regulator is used for the 2.5V and 3.3V supply voltage of the ADC used in the miniature camera. One of the regulators is used to provide 3.3V supply voltage of the digital level translator.

The other miniature power board is optimized for the supply power option. 6V supply voltage can be applied to the camera. In this board, the voltage converters are changed with the low dropout regulators. Therefore, eight low dropout regulators, namely LT1762, are used for the components and sensor in the camera.

Both of the boards are consist of two DACs, AD7399. They areserial input, quad, 10 bit DACs and directly programmed by FPGA. These DACsare used to provide analog bias voltages of the detector.

2.6.3 Miniature Digital Interface Board

Figure 2.21 shows the block diagram of the miniature digital interface board. Miniature digital interfaceboard is the thirdboard of the miniature camera system.The board consists of an FPGA, two low dropout regulators, an oscillator, and a microprocessor reset circuit.

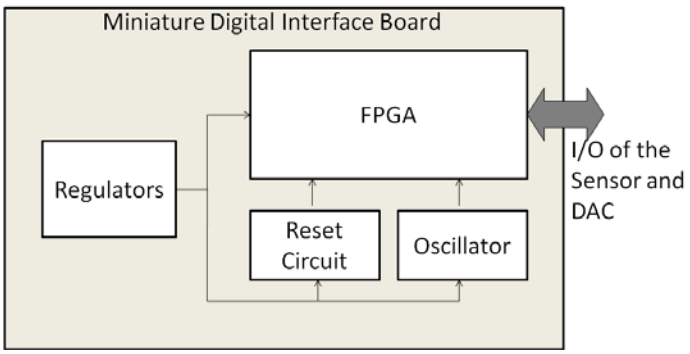


Figure 2.21: Block diagram of the miniature digital interface board.

ACTEL IGLOO nano series AGLN50V5-VQG250 FPGA is used in the miniature digital interface board as in the portable camera. It is a low power, small size, reprogrammable flash FPGA.Two regulators, namely LT3080,are used in theboard. It is a low dropout regulator with an output current of 1.1A. A 5V USB or supply voltage is applied to the input of one of the regulators, and 3.3V is produced for the FPGA. In addition, 3.3V DC voltage is applied to other regulator to produce 1.5V which is also for FPGA.

20 MHz TXC series clock oscillator is used in thisboard. Clock signal is provided to FPGA with the oscillator. 3.3V supply voltage of the oscillator is provided by the 3.3V low dropout regulator.

The microprocessor reset circuit, TS809, is used in thisboard to provide reset signal when the supply voltage decreases below the threshold value. The push button switch is not placed in thisboard because it is one of the middle boards in the miniature camera, and it is hard to push the button. Therefore, the push button reset switch is placed at the back side of the last board.

2.6.4 Miniature USB Communication Board

Figure 2.22 shows the block diagram of the USB communication board. The miniature USB communication board is the fourth and the last board of the miniature camera. In this board, there are a USB communication chip, a linear regulator, an EEPROM, a micro USB connector, a power connector, a power path controller, a programming header, and a reset switch.

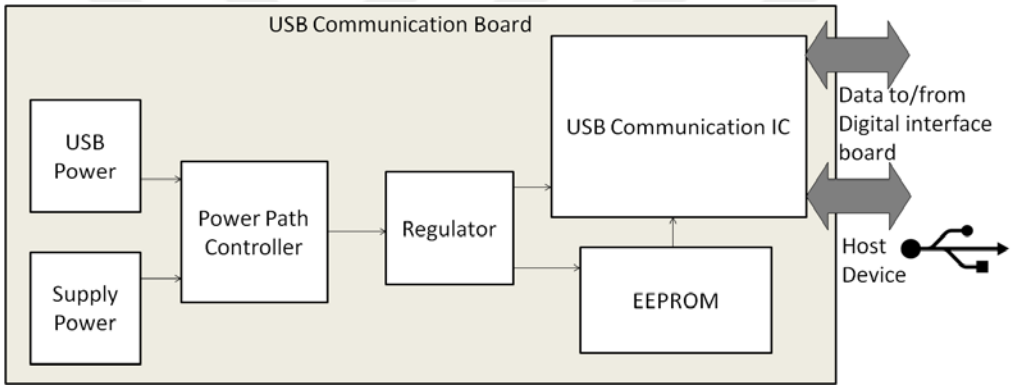


Figure 2.22: Block diagram of the USB communication board.

A USB communication chip, FT2232H, is used for the conversion of USB to UART interface. A direct communication with the UART interface and FPGA are provided through this chip. Alinear regulator, namely ADP124, is used to provide the 3.3V supply voltage of the USB communication chip. There is a 1.8V integrated low dropout regulator for the core in the FTDI chip.An external EEPROM is used for each of the channels of the chip for independent configuration. There are two different options to apply power to the USB communicationboard in the miniature camera: a micro USB connector and a power connector. These options are controlled by a power path controller,namely LTC4412, and it is used with a P-channel MOSFET to permit efficient OR'ing of different power sources.

A programming header is placed at the back side of the miniature USB communication board to program the FPGA in the thirdboard of the miniature camera with an external programming stick. Also, the push button reset switch is placed at the back side of theboard.

Table 2.2: Technical specifications of the miniature camera.

Miniature Camera	
Number of PCBs	4
Physical Dimension without Housing	$2.9 \times 2.9 \times 1.8 cm^3$
Physical Dimension with Housing	$3.1 \times 3.1 \times 3.1 cm^3$
Sensor	160 × 120 microbolometer
Power Signal	6V or USB power
Regulators	3 LT1762 low dropout regulators 5 TPS60241 voltage converters.
DACs	2 AD7399 10 bit, quad DACs. 1 LTC2640 10 bit DAC.
ADC	LTC2379 with series digital output and 1.6 MSPS conversion rate
Video Transfer	Via USB protocol
Power Dissipation	0.5 W

2.7 Camera Board Design

The layout design of the boards affects the performance of the camera as much as the circuit designs as discussed in Section 2.2. In this part, board layers and ground and power distribution will be discussed.

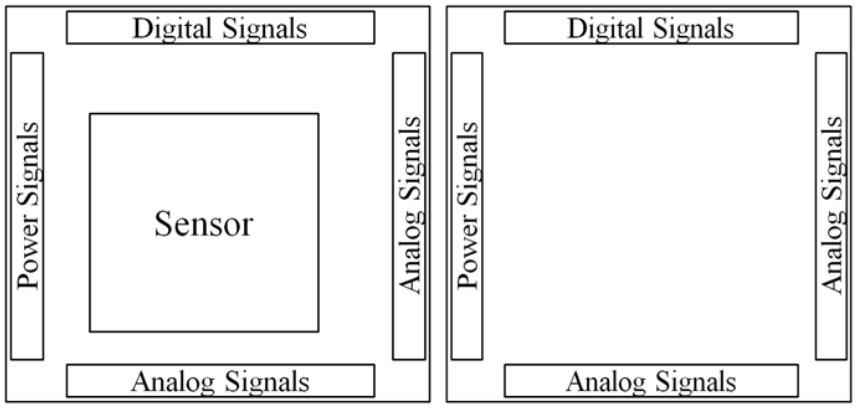
2.7.1 Board Layers

This section presents the boards of the portable and miniature camera. Section 2.7.1.1 and 2.7.1.2 show the board layers of the portable and miniature camera, respectively.

2.7.1.1 Board Layers of the Portable Camera

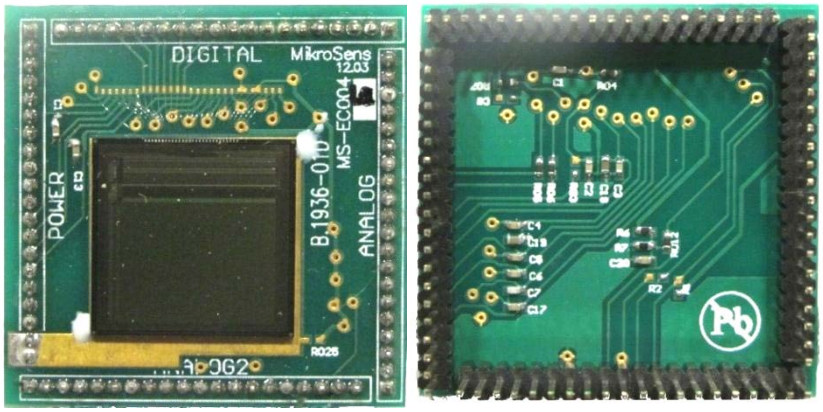
The portable camera has three boards: sensor interface board, camera electronics board, and digital interface and USB communication board. The sensor interface board and camera electronics board

have two layers. Figure 2.23 and Figure 2.24 show block again and photograph of both top and bottom sides of the sensor interface board of the portable camera, respectively. Figure 2.25 and Figure 2.26 show block diagram and photograph of both top and bottom sides of the camera electronics board of the portable camera, respectively



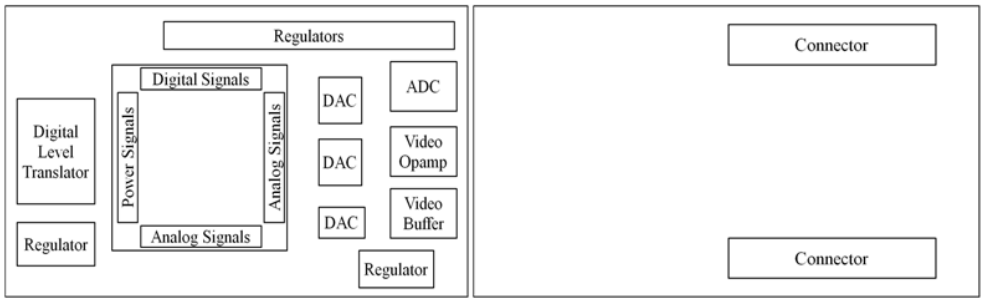
(a) (b)

Figure 2.23: Block diagram of the (a)top side, (b) bottom side of the sensor interface board of the portable camera.



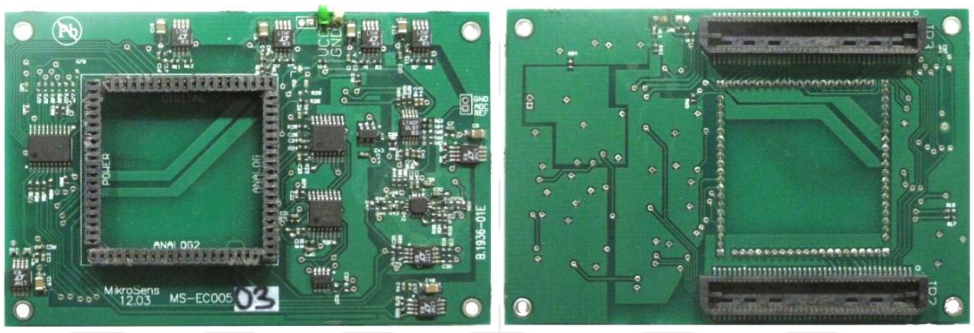
(a) (b)

Figure 2.24: Photograph of the (a)top side, (b) bottom side of the sensor interface board of the portable camera.



(a) (b)

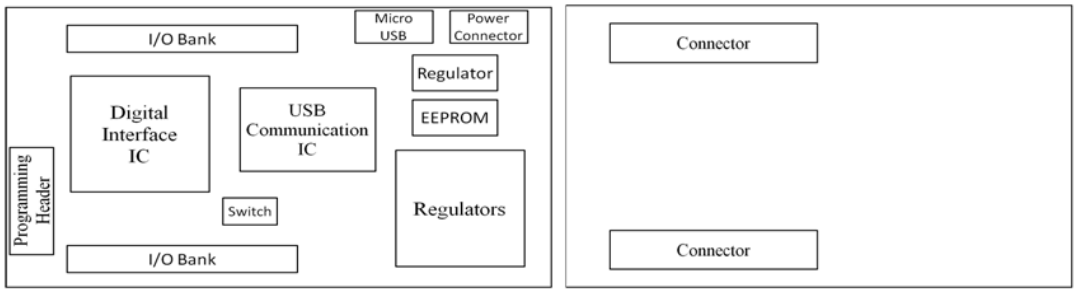
Figure 2.25: Block diagram of the (a) top side, (b) bottom side of the camera electronics board of the portable camera.



(a) (b)

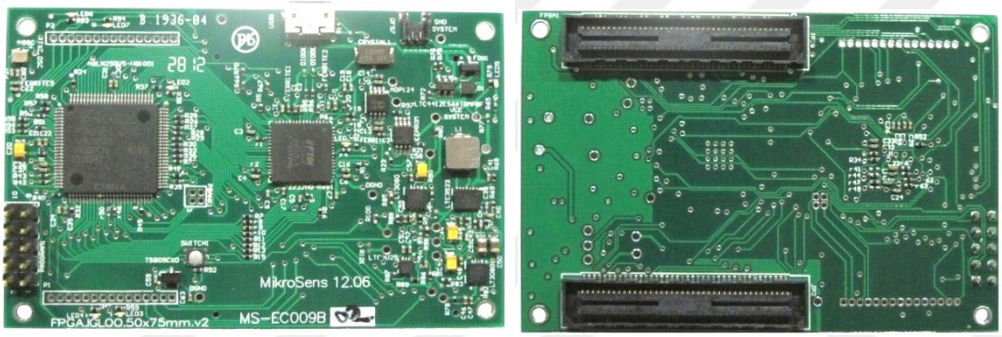
Figure 2.26: Photograph of the (a)top side, (b) bottom side of the camera electronics board of the portable camera.

The digital interface and USB communication board has four layers. Figure 2.27 and Figure 2.28 show the block diagram and photographs of both top and bottom side of the digital interface and USB communication board of the portable camera..



(a) (b)

Figure 2.27: Block diagram of the (a) top side, (b) bottom side of the digital interface and USB communication board of the portable camera.

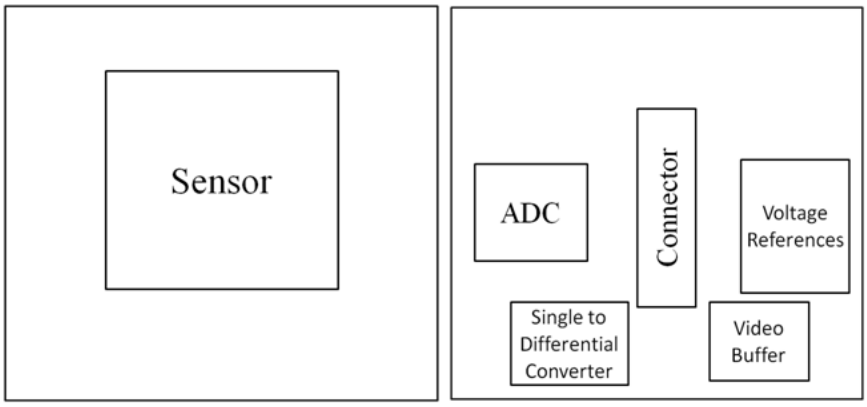


(a) (b)

Figure 2.28: Photograph of the (a) top side, (b) bottom side of the digital interface and USB communication board of the portable camera.

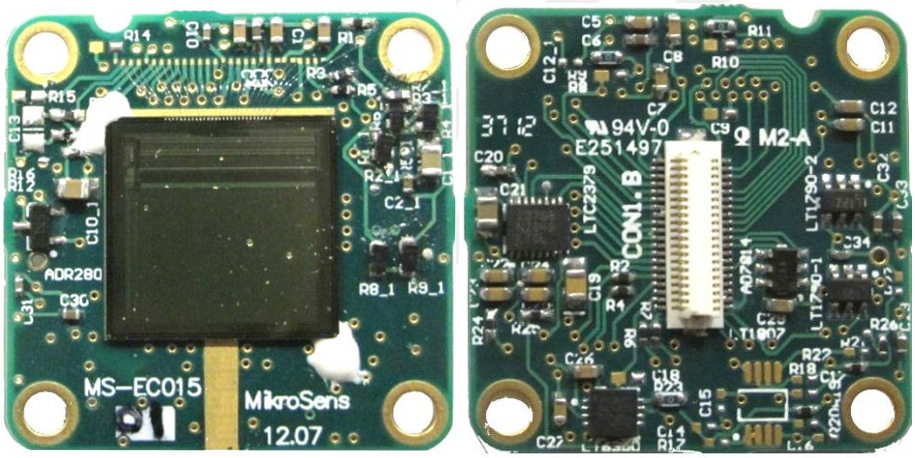
2.7.1.2 Board Layers of the Miniature Camera

The miniature camera boards: sensor interface board, power board, digital interface board, and USB communication board have six layers, and Figure 2.29 and Figure 2.30 show the block diagram and photographs of both top and bottom side of the sensor interface of the miniature camera, respectively. In addition, Figure 2.31 and Figure 2.32 show the block diagram and photographs of both top and bottom side of the power board of the miniature camera, respectively.



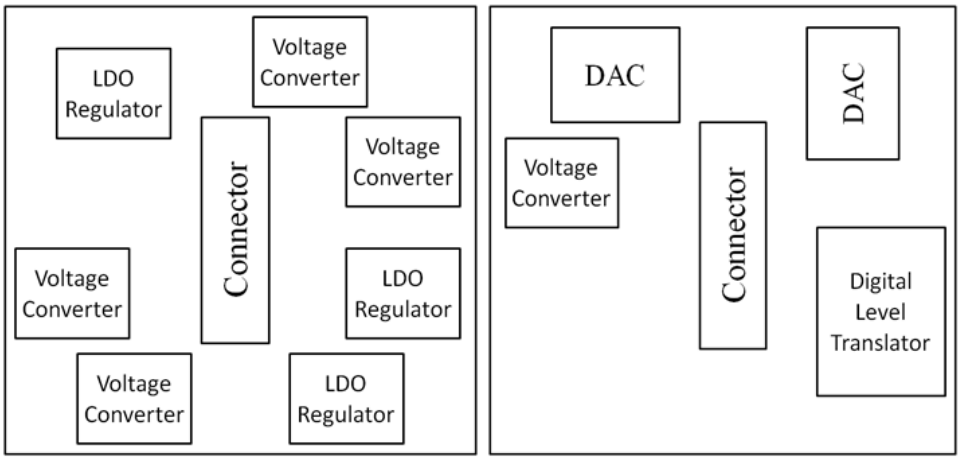
(a) (b)

Figure 2.29: Block diagram of the (a) top side, (b) bottom side of the sensor interface board of the miniature camera.



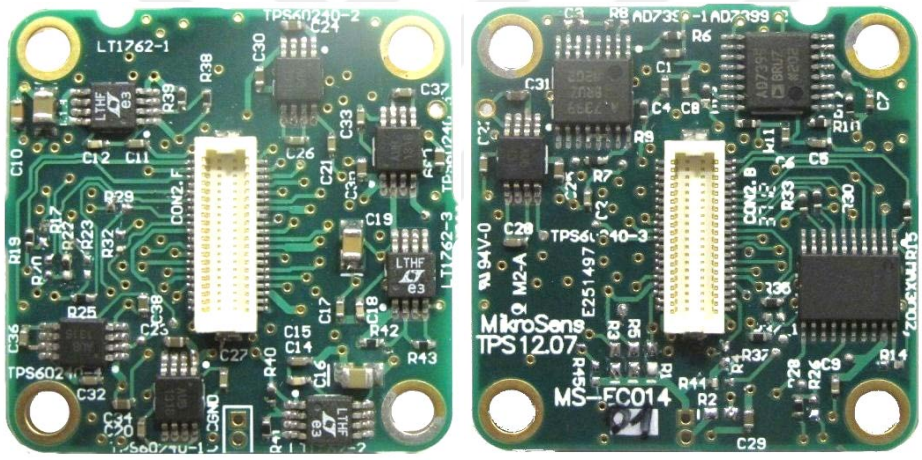
(a) (b)

Figure 2.30: Photograph of the (a) top layer, (b) bottom layer of the sensor interface board of the miniature camera.



(a) (b)

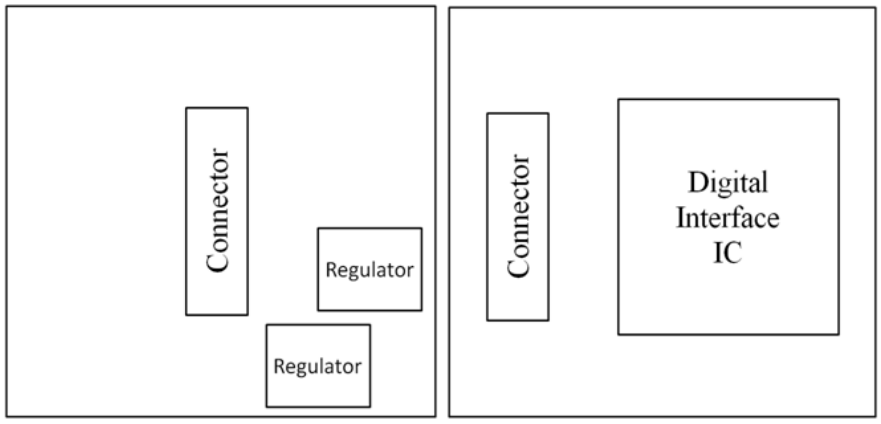
Figure 2.31: Block diagram of the (a) top side, (b) bottom side of the power board of the miniature camera.



(a) (b)

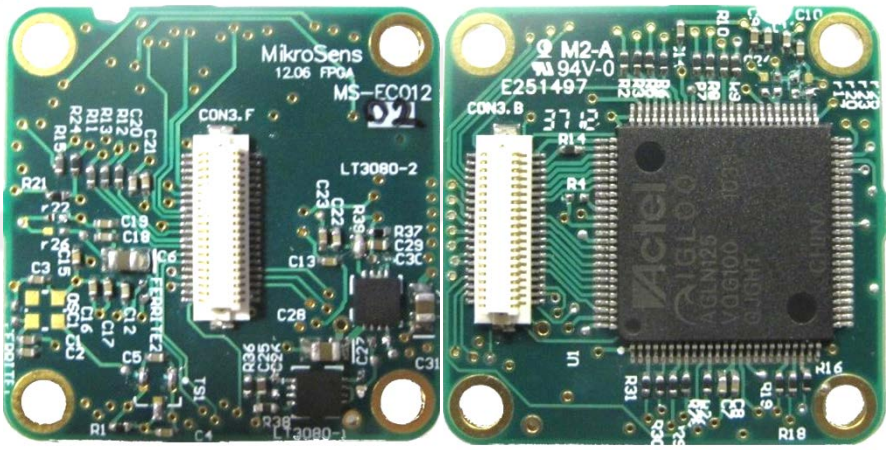
Figure 2.32: Photograph of the (a) top layer, (b) bottom layer of the power board of the miniature camera.

Furthermore, both the digital interface and the USB communication boards have six layers in miniature camera. Figure 2.33and Figure 2.34show the block diagram and photographs of both top and bottom side of the digital interface board of the miniature camera, respectively. Figure 2.35 and Figure 2.36show the block diagram and photographs of both top and bottom side of the USB communication board of the miniature camera, respectively.



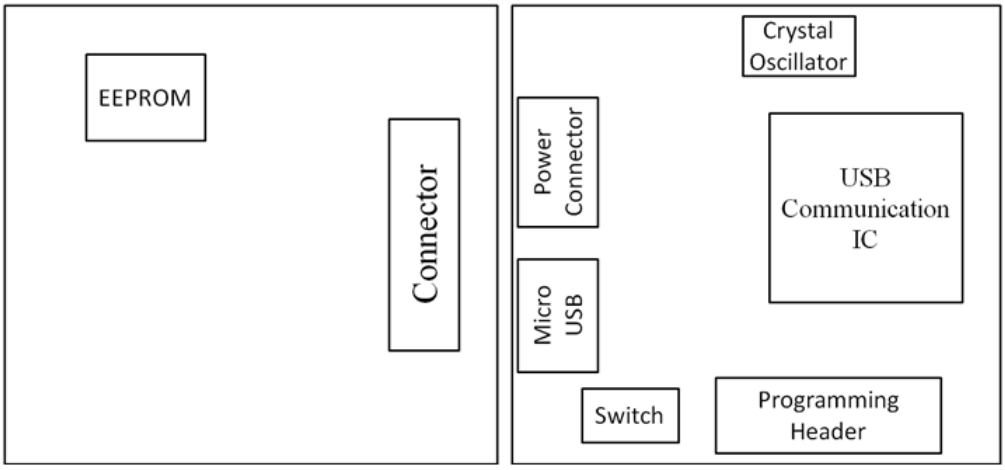
(a) (b)

Figure 2.33: Block diagram of the (a) top side, (b) bottom side of the digital interface board of the miniature camera.



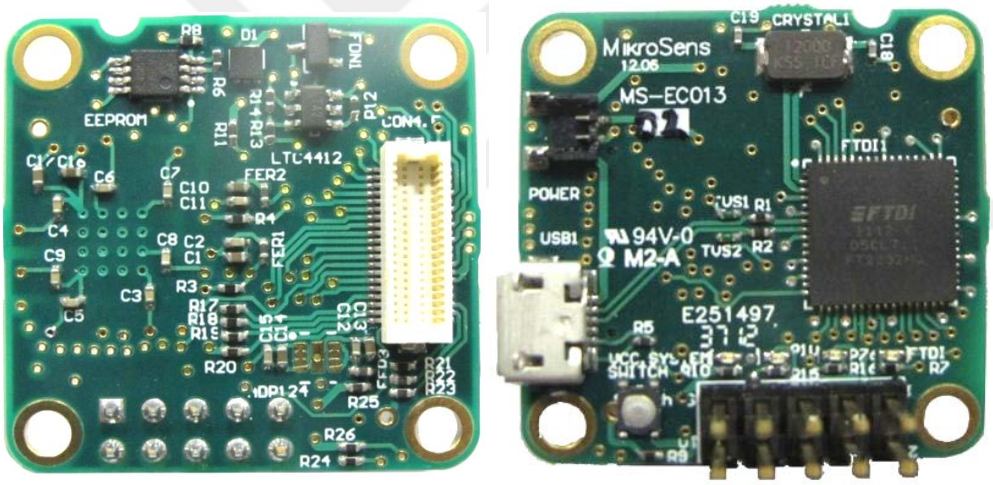
(a) (b)

Figure 2.34: Photograph of the (a) top layer, (b) bottom layer of the digital interface board of the miniature camera.



(a) (b)

Figure 2.35: Block diagram of the (a) top side, (b) bottom side of the USB communication boardof the miniature camera.



(a) (b)

Figure 2.36: Photograph of the (a) top layer, (b) bottom layer of USB communication board of the miniature camera.

2.7.2 Ground and Power Distribution

Ground and power distribution of the camera affects the camera performance. The main idea is to separate the power signals of different blocks as much as possible and star connect them in the lowest impedance node so that the different components do not cross talk between each other via the power The ground and power distribution of both portable and miniature camera will be discussed in Section2.7.2.1 and 2.7.2.2 in detail.

2.7.2.1 Ground and Power Distribution of the Portable Camera

In the portable camera the ground and supply voltages are applied from the camera electronics board. Analog and digital ground planes are separated from the ground and they are distributed to the sensor interface card. Figure 2.37 shows the ground distribution of the portable camera electronics.

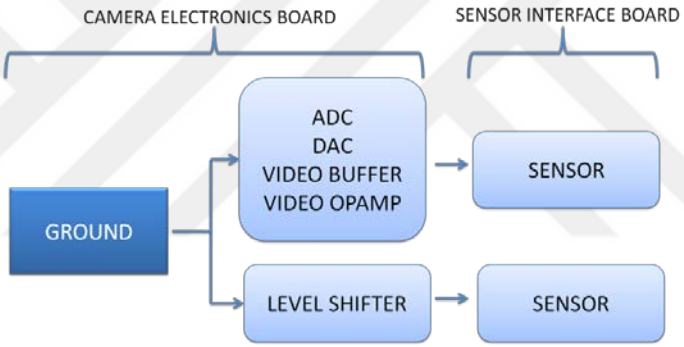


Figure 2.37: Ground distribution of the portable camera electronics.

Supply voltage is applied from the camera electronics board, and it directly goes to the inputs of the regulators in the same board. All of the camera electronics are in the same board except the sensor. Analog and digital supply voltages of the sensor are distributed to the sensor interface board with connectors. Figure 2.38 shows the power distribution of the portable camera electronics.

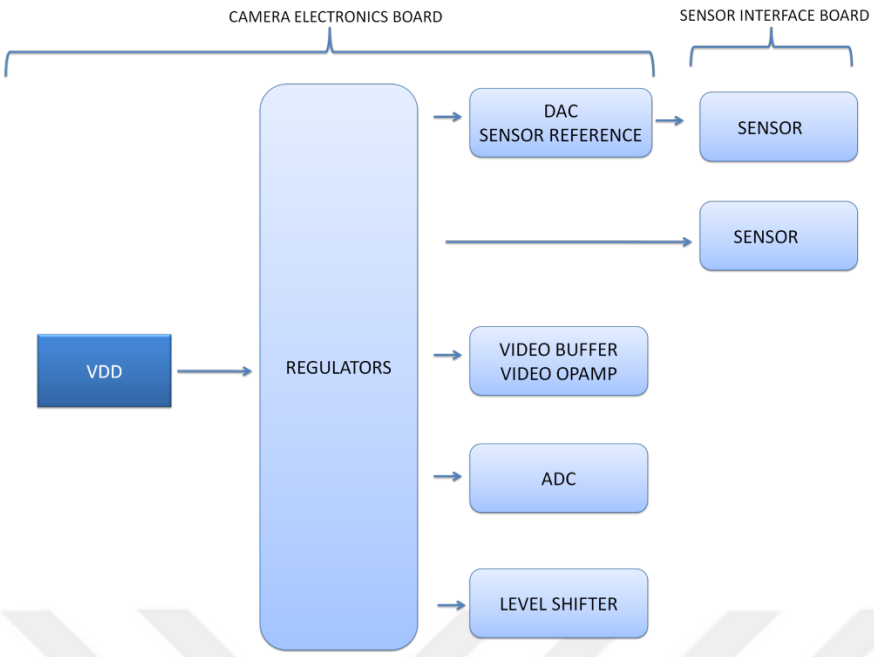


Figure 2.38: Power distribution of the portable camera electronics.

2.7.2.2 Ground and Power Distribution of the Miniature Camera

The miniature camera is powered up through either USB or supply power. The ground and supply voltage is applied through the USB communication board of the camera. Figure 2.39 shows the ground distribution of the USB powered miniature camera electronics

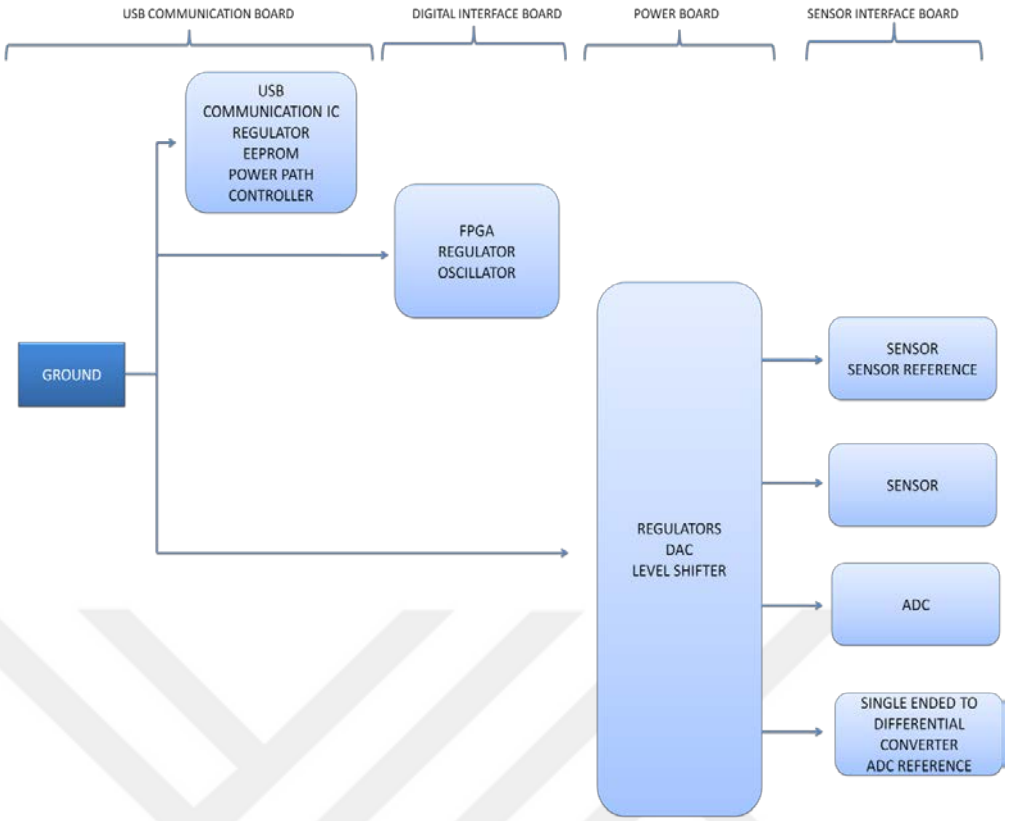


Figure 2.39: Ground distribution of the USB powered miniature camera electronics.

The supply voltage of the camera is applied and distributed from the USB communication board to the sensor interface board. Figure 2.40 shows the power distribution of the miniature camera electronics.

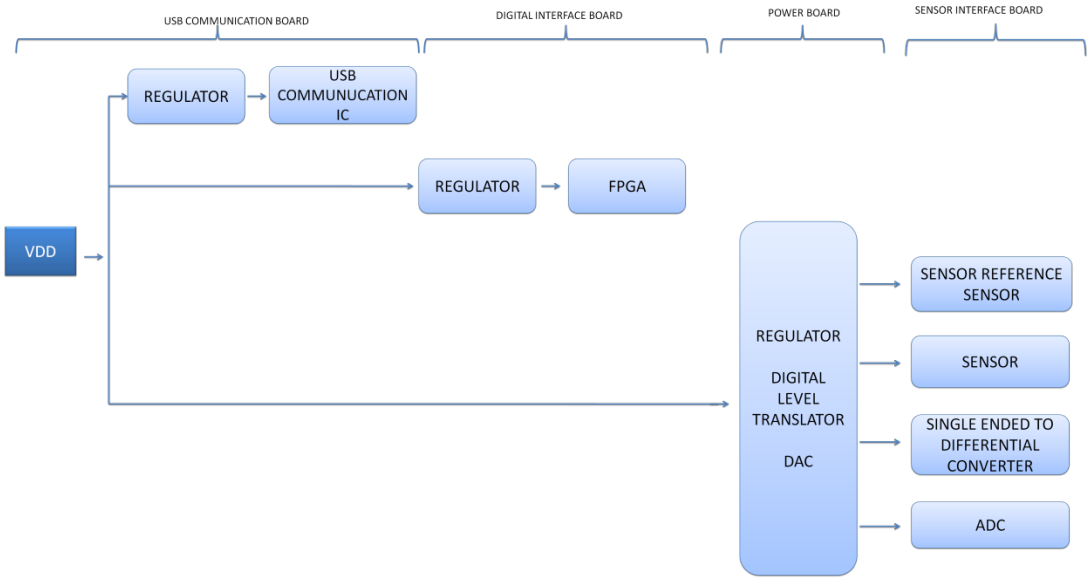


Figure 2.40: Power distribution of the miniature camera electronics.

2.8 Conclusion

This chapter summarizes the camera electronics of the low-cost uncooled microbolometers. Firstly,the design guidelines for high performance camera electronics are discussed.Then, the previous works completed at METU-MEMS Center is presented. The chapter continues by describing the camera electronics for both portable and miniature camera. Design procedure of each board consisting the camera is explained individually. Furthermore, board layers and the ground and power distribution of the cameras is presented.

CHAPTER 3

IMPLEMENTATION

3.1 Introduction

This chapter explains the implementation of each camera in detail. Although camera electronics design is the main focus of this thesis, the mechanical design is also crucial to assemblea camera from electronic components. This chapter first discusses the mechanical design of the cameras. The mechanical design of each camera includes stacking of the boards are presented with the 3D views of the cameras. Both portable and miniature cameras havemultiple camera boards. All of the boards are stacked with connectors to form a handheld camera. In addition to this, housing and optical mounts of the housing are critical to get the IR images. Housing of the cameras has optical mount parts to fix the lens to the camera, and the lens should come right on top of the optic center of the detector

3.2 Mechanical Design

This section briefly explains the mechanical design of the board stack of the cameras.

3.2.1 Mechanical Design of the Portable Camera

In the portable camera electronics, there are three boards: sensor interface, camera electronics, and digital interface and USB communication boards. The sensor interface board covers an area of 3×3 cm^2, and the camera electronics and digital interface and USB communication boards cover 5x7.5 cm^2. The sensor interface board and the camera electronics board are stacked on each other with HARWIN M52 series connectors. In addition, the camera electronics board and the digital interface and USB communication boards are stacked with the Samtec BSE-040-01-F-D-A and Samtec BTE-040-01-F-D-A connectors. Figure 3.1 andFigure 3.2shows the mechanical design and the photograph of the portable camera, respectively.

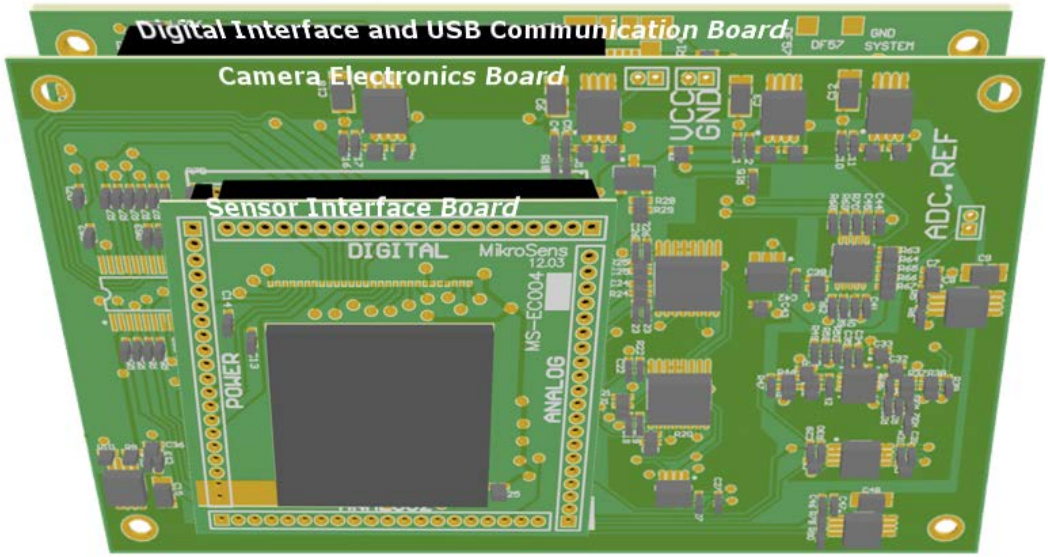


Figure 3.1: Mechanical design of the portable camera.

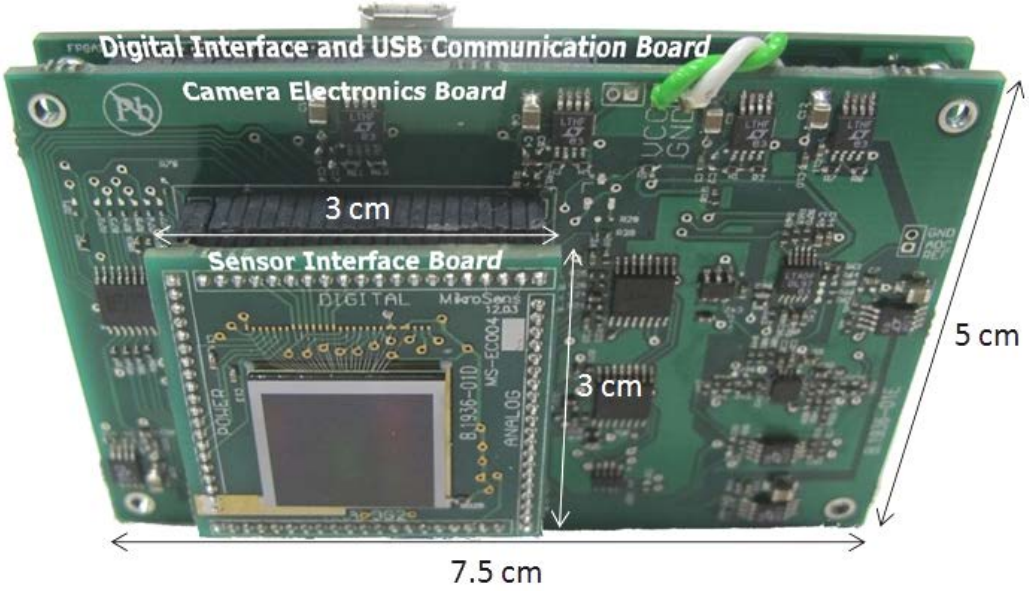


Figure 3.2: Photograph of the portable camera.

3.2.2 Mechanical Design of the Miniature Camera

The miniature camera is consists of four boards: sensor interface board, power board, digital interface board, and USB communication board. Four of the boards are connected using HIROSE DF12 series, 0.5mm pitch SMT board to board connector. It is an ultra-miniature size connector with a stacking height of 3.5mm, and it has 40 contacts in two rows. It occupies an area of 12.1×9.5mm^2.Figure 3.3and Figure 3.4 show the mechanical design and photograph of the miniature camera.

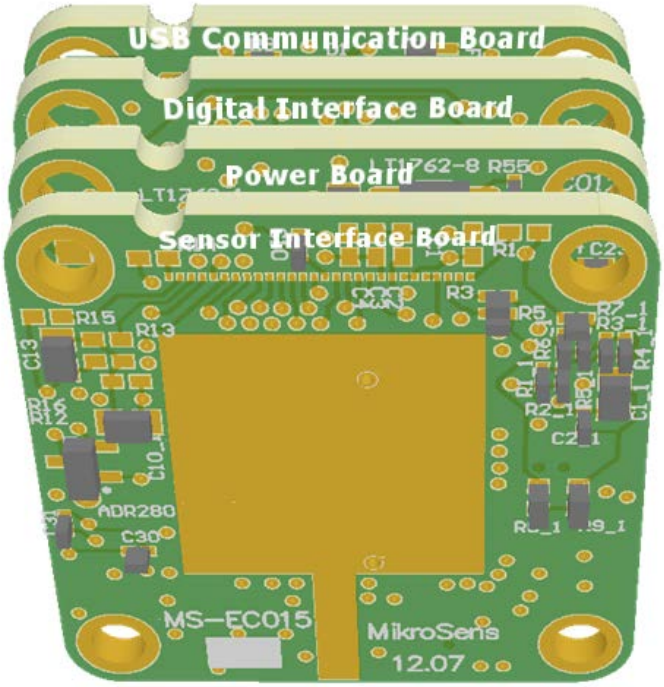


Figure 3.3: Mechanical design of the miniature camera.

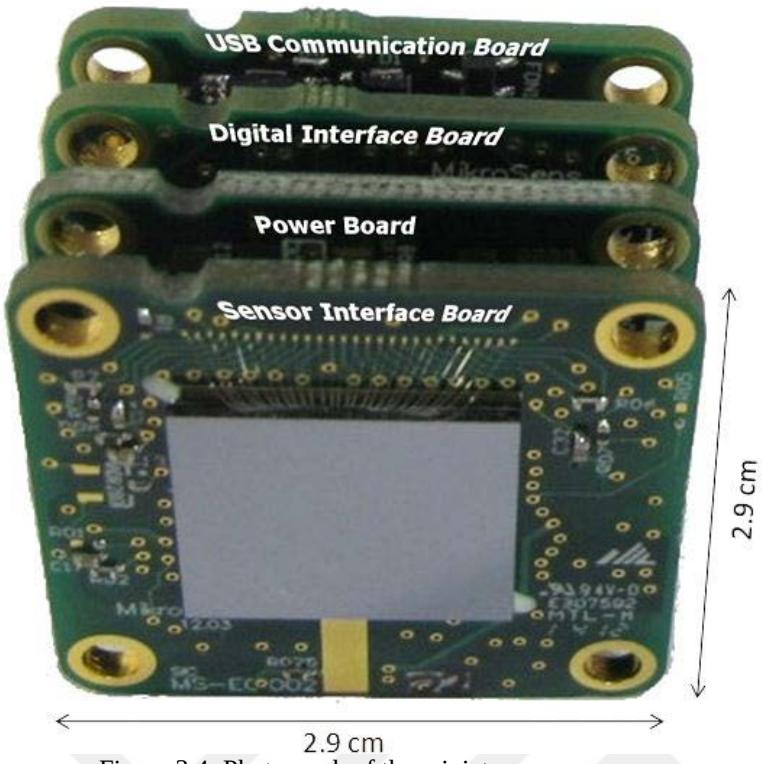


Figure 3.4: Photograph of the miniature camera.

3.3 Housing and Optics

Housing and lenses are important parts of a camera system for achieving a handheld camera. A metal case which covers the electronics boards and carries the optical lens is designed for portable camera electronics. Figure 3.5 shows this housing of the portable camera. The dimension of the housing is $7.9\times5.4\times2.2cm^3$ without lens. The depth of the housing and the internal connection points are adjusted so that the infrared sensor chip is placed at the focal plane and optical center of the lens.



Figure 3.5: Housing of the portable camera. The dimension of the housing is 7.9x5.4x2.2cm^3 without lens.

Furthermore, a different housing is designed for the miniature cameras. Figure 3.6 shows the housing of the miniature camera. The dimensions of the housing are 3.1×3.1×3.1cm^3 without lens. This housing is designed considering the optical center and the focal length of the lens.



Figure 3.6: Housing of the miniature camera. The dimension of the housing is 3.1×3.1×3.1cm^3 without lens.

The optics of the camera systems is fitted to the optical mount of the housings as shown in Figure 3.5 and Figure 3.6. In the thermal camera systems, a lens with the infrared-transmitting material should be used.Lens materials, f-number, and focal length are very important parameters while choosing a lens for the camera system.

During the last decade, new infrared materials have grown up to decrease the cost of the infrared camera systems. Lens is one of the most important limitationsto decrease the cost of the infrared camera systems. Germanium lenses are used traditionally for the infrared systems, and they are high performance lenses. Their transmission windowis 0.8µm to 16 µm. The mechanical resistance of germanium lenses is very high. Also, the refractive index of germanium is 4.0. Higher refractive index is an advantage because, it blocks the higher aberrations. On the other hand, disadvantage of germanium lenses is the cost which is one of the most important criteria for the thermal imaging systems.GASIR lenses are a type of chalcogenide lenses. These lenses are a new type of an infrared material. Their transmission window is 0.8 µm to 14 µm and the refractive index is 2.5. The most important advantage of the GASIR lenses is their lower cost.

The focal length of a lens is defined by the required field of view of the camera and the size of the detector [33]. The ratio of the focal length of a lens to the diameter of the lens is the f-number of the lens. F-number of lenses affects the sensitivity of the camera system, because it determines the light gathering power of the lens. [34].

Angle of view of a lens is determined from the focal length of the lens. Short focal length lenses have a wide angle of view, on the other hand, long focal length lenses have narrow angle of view.In addition, the back distance is another parameter and it affecting the camera size. Back distance of the lens is the distance between the sensor and the lens.

In the designed cameras, GASIR lenses are preferred because of the cost. These lenses with the 8.52 mm focal length and 1.24 f number can be used in this system [35]. Image circle of 14mm is guaranteed and it is suitable for the 160×120 microbolometer. In addition, lenses with the 10.3 mm focal length and 1.25 f number can be used. The maximum image circle of these lenses 12 mm and they also covers the FPA of the sensor.

3.4 Conclusion

Implementation of the designed camera electronics are described in this chapter. Firstly, mechanical designs of the camera electronics are explained, and 3-D views of the portable and miniature camera are shown. In the portable camera, there are three boards and two types of connectors are used to stack theseboards. The mechanical design of the miniature camera is relatively different and challenging. The size of the camera is ultra small. Therefore, miniature connectors should be used to stackfour different boards to form the camera. Furthermore, housing and optics of the cameras are summarized at the end of this chapter.

CHAPTER 4

TEST RESULTS

4.1 Introduction

In this chapter, the test results of the designed camera electronics will be presentedin order to provide a measure of their performances, noise levels and power consumptions. In the tests, the camera boardsand a computer are used. In addition to that, the portable camera which is not a USB powered system, require an external power supply.

In the tests of the camera electronics, first the analog signal chain noise, and then the noise of the whole system including the imager was measured. The analog signal chain noise is measured by applying a fixed DC voltage between the differential inputs of the ADCs, and the common mode noise that applies to both the voltage supply and ADC is cancelled differentially because of the differential inputs.

The performance of the imager is affected by the noise of the readout electronics, which is also a function of the noise of the circuit that powers it. Figure 4.1 shows the simplified block diagram of the readout electronics of the 160×120 microbolometer. If there is no infrared radiation absorbed by the detector, the voltage drop on the constant current biased pixel and the reference pixel are same. Therefore, there is no current flow to the amplifier. If the detector absorbs infrared radiation, voltage drop on the pixel is increased, and it generates a current flow to the amplifier.

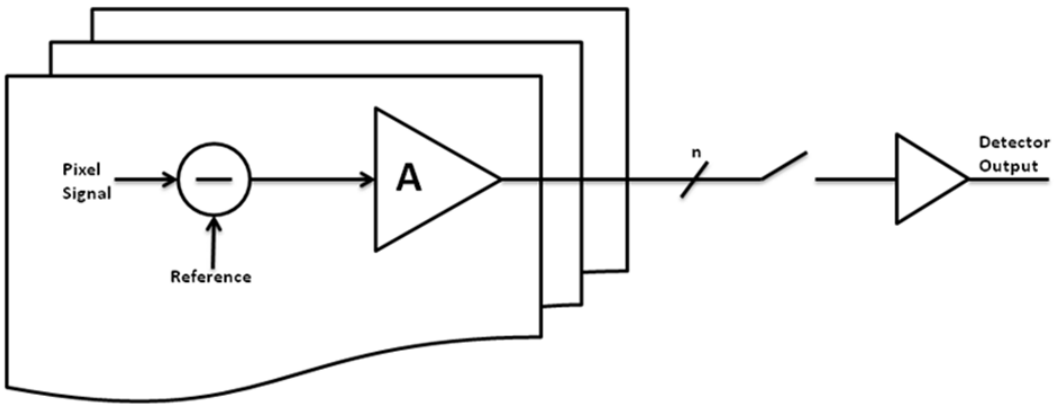


Figure 4.1: A simplified block diagram of the readout electronics of the 160×120 microbolometer.

As seen on the simplified block diagram, there is an amplifier with a gain of A in the ROIC in order to amplify the detector signal. If the gain of the amplifier is zero, the noise of the system with the detector is measured with the name of zero gain noise.Measuring the noise with zero gain will provide a means to characterize the system performance independent from the noise induced by the pixels. In addition, the noise of both the detector and the camera electronics are measured with the name of fixed gain noise. Fixed gain noise is the final measure of the overall system performance. The noise measurements include 64 consecutive frames data, and the data is analyzed by MATLAB.

Size is one of the main focuses of this thesis. The portable camera is designed to have the first compact camera, and miniature camera is designed to have the maximum portability

Furthermore, power dissipation is another performance parameter for the designed camera electronics. Power dissipation of each of the designed camera is measured with and without sensor.

4.2 Portable Camera

This section presents the test results of the portable camera electronic. Figure 4.2 shows the test setup for the portable camera. The test setup consists of a low noise DC power supply, a computer, and the portable camera.

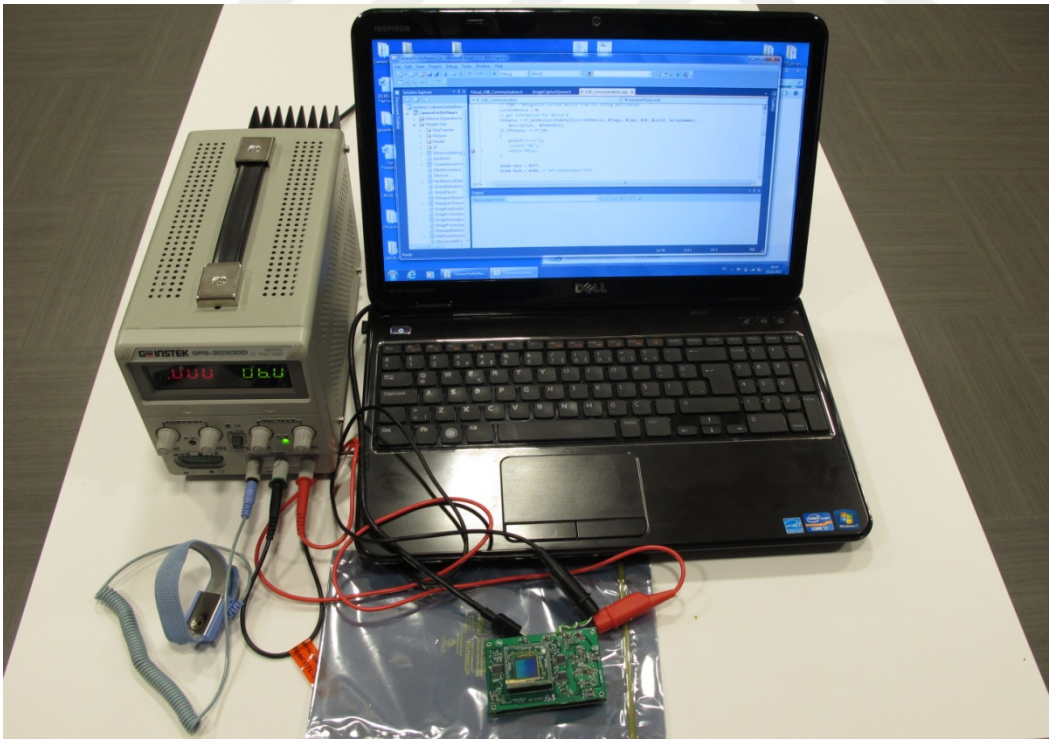


Figure 4.2: The test setup for the portable camera. The test setup consists of a low noise DC power supply, a computer, and the portable camera.

The signal chain noise measurement consists of accumulation of noises of the video buffer, the video opamp, and the ADC. The inputs of the dual video buffer are the analog output of the sensor and a common mode voltage applied by a DAC. Firstly, the sensor interface board of the camera is disconnected from the camera, and the digital outputs of the sensor are imitated and applied by FPGA. The DAC output is short circuited with the analog output of the sensor. The combination of video buffer, video opamp, and ADC noise is measured with this method. Figure 4.3 shows the signal chain noise histogram of the portable camera. The average noise is 2.9 ADC count with 14 -bit ADC which corresponds to 0.44m V_{RMS}. The signal chain noise is calculated as 1.43 ADC count with 14-bit ADC from datasheets of the components that are used in the portable camera. The difference between the calculation and measurement may be caused by the layout of the boards. The camera electronics board of the portable camera has 2layers. Therefore, ground and power routings have higher impedances compared to4-layer PCBs.

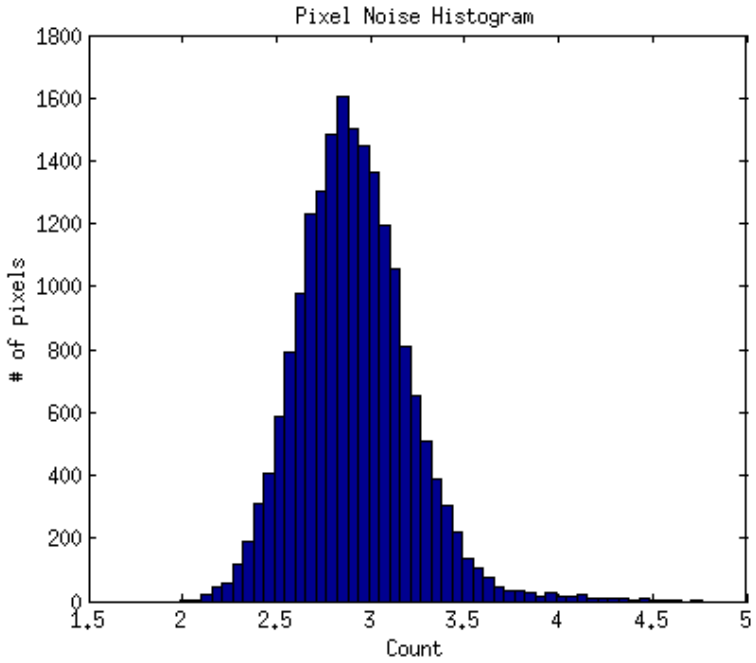


Figure 4.3: Signal chain noise histogram of the portable camera. The average noise is 2.9 ADC count with 14-bit ADC which corresponds to 0.44m V_{RMS}.

Then, sensor is connected from the camera and fixed gain of the detector, which is described in the Section 4.1, is shut down. The measurement is similar with the signal chain noise. Figure 4.4 shows the zero gain noise histogram of the portable camera. The average noise is 3.1 ADC count with 14-bit ADC which corresponds to 0.47m V_{RMS}..

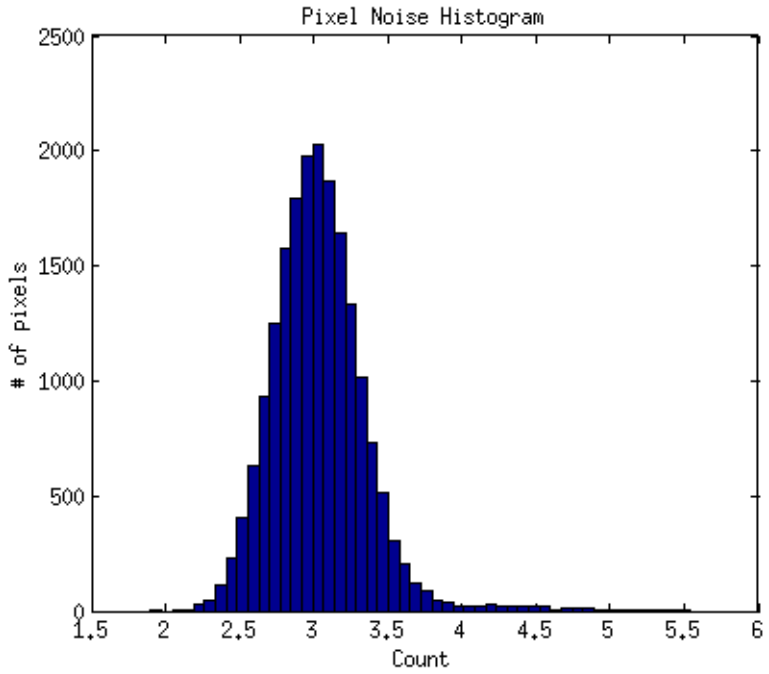


Figure 4.4: Zero gain noise histogram of the portable camera. The average noise is 3.1 ADC count with 14-bit ADC which corresponds to 0.47m V_{RMS}.

Finally, the total noise of the portable camera is measured. The total noise includes the detector noise in addition to the previous measurement. Figure 4.5shows the detector noise histogram of the portable camera. The average noise is 10.2 ADC counts with 14-bit ADC which corresponds to 1.56m V_{RMS}. There are two different peaks in the noise histogram. It is because of the detector characteristics. There is an additional noise source in the spectrum of SOI medium thickness transistors [38], and it considerably affects the system noise.

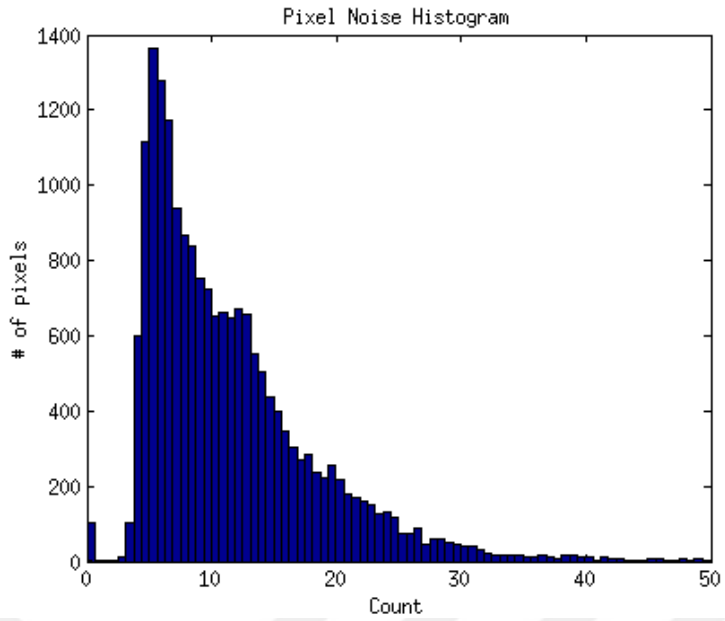


Figure 4.5: Detector noise histogram of the portable camera. The average noise is 10.2 ADC counts with 14-bit ADC which corresponds to 1.56m V_{RMS}.

The power dissipation of the camera is also measured. The power consumption of the camera electronics is 0.15 Watts without the sensor and 0.2 Watts with sensor. Also, the digital interface and USB communication board has a power dissipation of 0.4Watts.Table 4.1shows the features of the portable camera.

Table 4.1: Features of the portable camera.

Features of the Portable Camera	
Signal Chain Noise	0.44 mV_{RMS}
Zero Gain Noise	0.47 mV_{RMS}
Noise of the System with Fixed Sensor Gain	1.56 mV_{RMS}
Size Without Housing	$7.5\times5\times2\ cm^3$
Size With Housing	$7.9\times5.4\times2.2\ cm^3$
Power Dissipation Without Sensor	0.55 Watts
Power Dissipation With Sensor	0.6 Watts

4.3 Miniature Camera

The miniature camera consists of the miniature sensor interface board, power board, digital interfaceboard, and USB communicationboard. The camera system is tested with both the USB and supply power options. As described in the Chapter 2, there is a power path controller in the miniature USB communicationboard of the camera. USB cable plugged to the board, and data transfer between the digital interface IC and the computer is done with the USB connection. However, if supply power is applied from the power connector, the power path controller chooses the supply power. If the supply power is not applied from the power connector, camera will work with the USB power. Figure 4.6 and Figure 4.7 show the test setup for the DC supply powered and USB powered miniature camera, respectively.



Figure 4.6: Test setup for the DC supply powered miniature camera. The test setup consists of a low noise DC power supply, a computer, and the miniature camera.

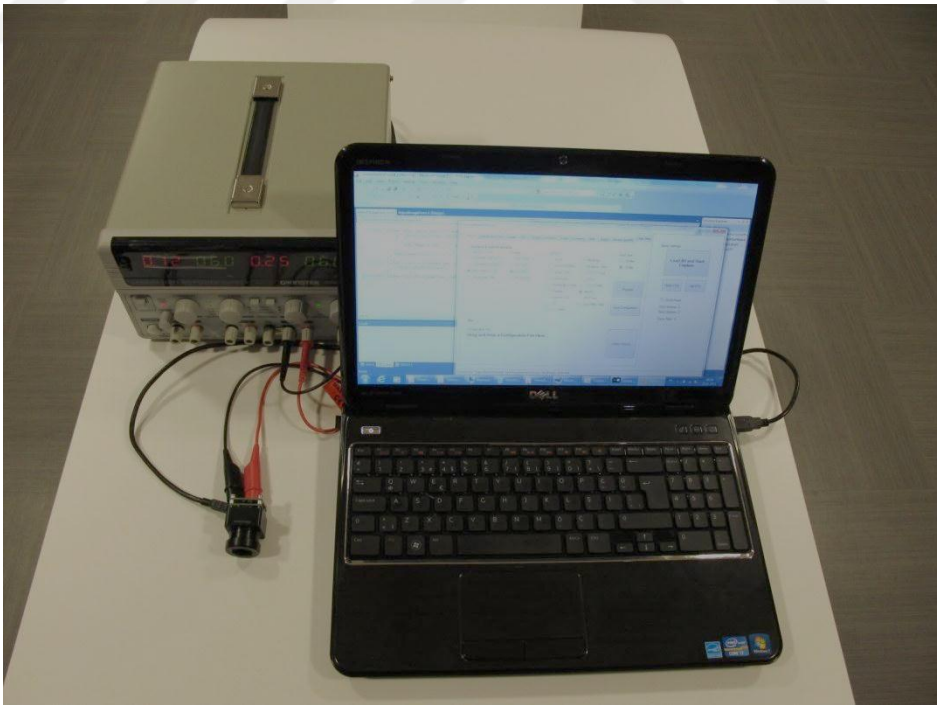


Figure 4.7: Test setup for the USB powered miniature camera. The test setup consists of a computer and the miniature camera.

Firstly, the tests are done with the supply poweroptimized miniature power board. In this camera system, there is a single to differential converter and an 18 bit ADC. Normally, one of the inputs of the single to differential converter is the analog output of the sensor, and the other input is a common mode voltage applied by a voltage reference. A differential signal is created from the analog output of the sensor with respect to the common mode voltage, and fully differential signals are the inputs of the ADC. Signal chain noise measurement is done before the wire-bonding of the sensor to the sensor interface board of the camera and the inputs of the single to differential converter are shorted to the signal applied by the voltage reference.

The measurement is done with this power board and supply power. Figure 4.8 shows the signal chain noise histogram of the miniature camera with supply power. The average noise is 1 ADC count with 18-bit ADC which corresponds to 19µ V_{RMS}. The signal chain noise is calculated as 0.97 ADC count with 18-bit ADC from datasheets of the components that are used in the miniature camera. The measured noise is very similar with the calculated noise. Because the miniature camera has 6-layer boards, and low impedance power and ground planes are used to minimize the noise.

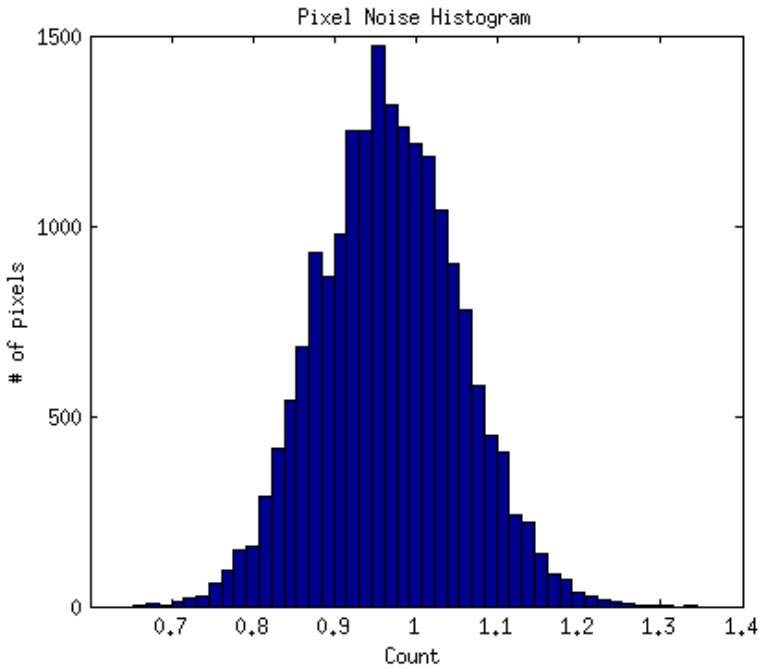


Figure 4.8: Signal chain noise histogram of the miniature camera with supply power. The average noise is 1 ADC count with 18-bit ADC which corresponds to 19µ V_{RMS}.

Then the signal chain noise is measured with the USB power optimized miniature power board and USB power. The signal chain noise is measured with the same method. The inputs of the single to differential converter are shorted and the voltage is applied from the voltage reference. Figure 4.9 shows the signal chain noise histogram of the miniature camera with USB power. The average

noise is 1.2 ADC count with 18-bit ADC which corresponds to 23µ V_{RMS}.The difference between the signal chain noises of supply powered and USB powered miniature cameras caused by the glitches of the USB power signals as described in Section 2.2.6.

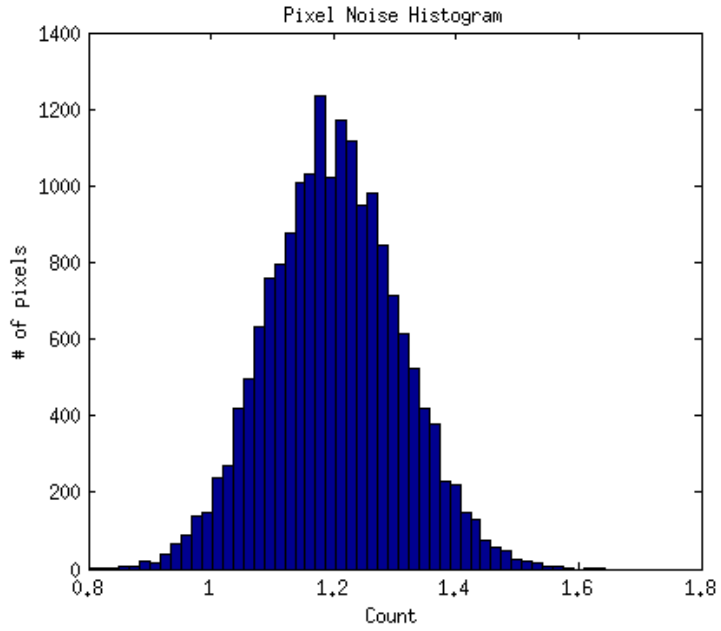


Figure 4.9: Signal chain noise histogram of the miniature camera with USB power. The average noise is 1.2ADC count with 18-bit ADC which corresponds to 23µ V_{RMS}.

After the measurements of the signal chain noise, sensor is wire-bonded to the sensor interface boardand thezero gain noise is measured. The result of the zero gain noise with the supply power optimized miniature power board, and Figure 4.10 shows the zero gain noise histogram of the miniature camera with supply power. The average noise is 4.3 ADC count with 18-bit ADC which corresponds to 0.08m V_{RMS}

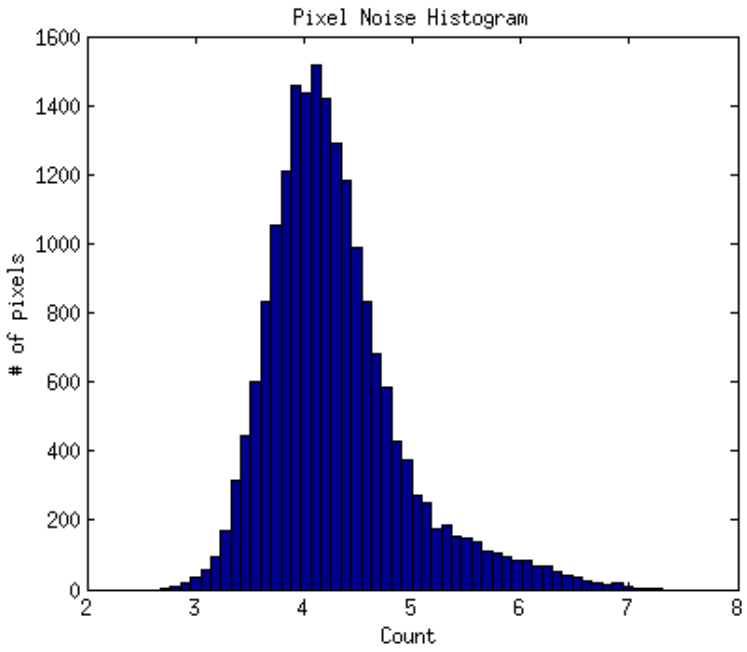


Figure 4.10: Zero gain noise histogram of the miniature camera with supply power. The average noise is 4.3 ADC count with 18-bit ADC which corresponds to 0.08m V_{RMS}.

Also, one more zero gain measurement is done with the USB power optimized miniature power board with USB powered. Figure 4.11 shows the zero gain noise histogram of the miniature camera with USB power. The average noise is 9.1 ADC count with 18-bit ADC which corresponds to 0.17m $V_{RMS.}$

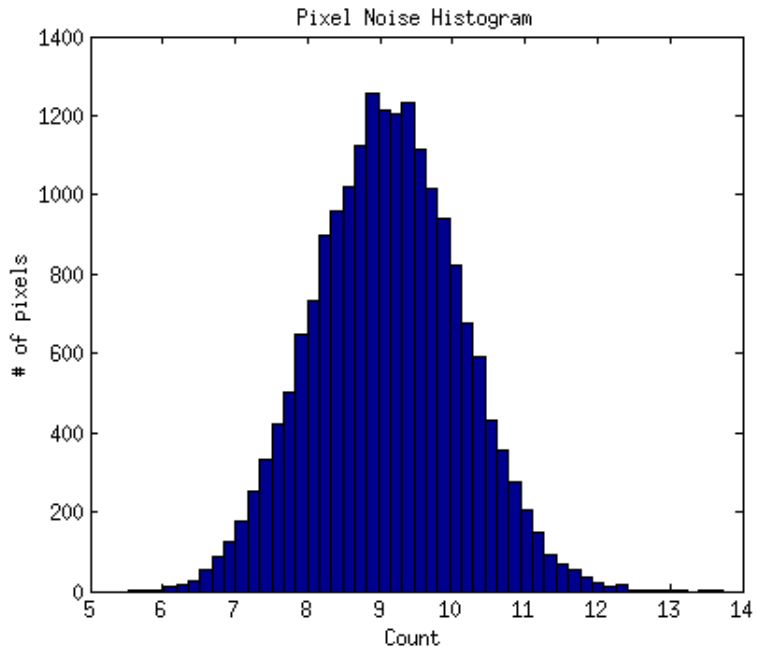


Figure 4.11: Zero gain noise histogram of the miniature camera with USB power. The average noise is 9.1 ADC count with 18-bit ADC which corresponds to 0.17m V_{RMS}.

Furthermore, sensor noise is measured with both of the miniature power boards. The noise is measured as 3.53m V_{RMS} which is 185 ADC counts with the miniature power board and supply power. Also, the noise measurement with the miniature power board and USB power is done and the result is 3.62m V_{RMS} which is 190 ADC counts. Figure 4.12 shows the detector noise histogram of the miniature camera with supply power. The average noise is 185 ADC count with 18-bit ADC which corresponds to 3.53m V_{RMS}. In the noise histogram, there is a peak that is around 0 count noise level which is caused by the saturated pixels. Figure 4.13 shows the detector noise histogram of the miniature camera with USB power. The average noise is 190 ADC count with 18-bit ADC which corresponds to 3.62m V_{RMS}. The noise histogram of the detector has more than one peak because of the additional noise contribution of the detectors described in Section 4.2.

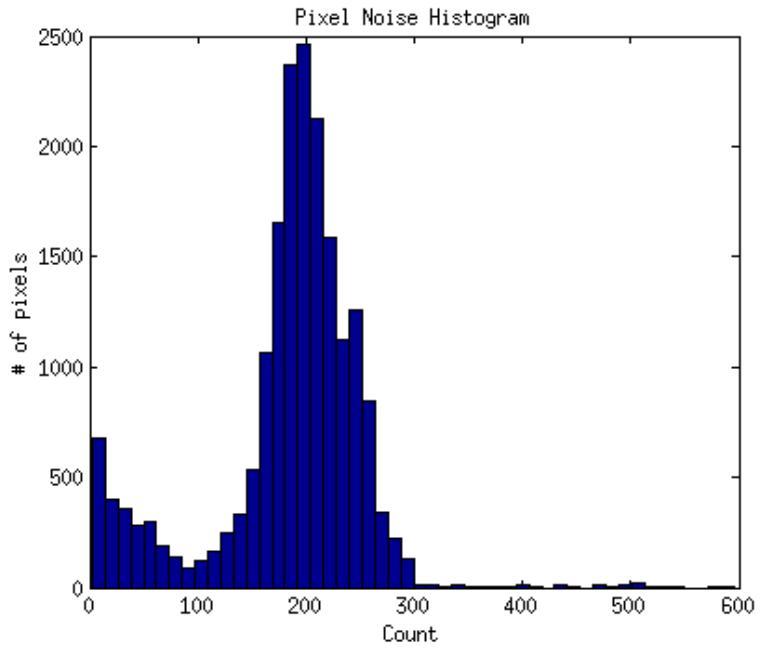


Figure 4.12: Detector noise histogram of the miniature camera with supply power. The average noise is 185 ADC countwith 18-bit ADC which corresponds to 3.53m V_{RMS}.

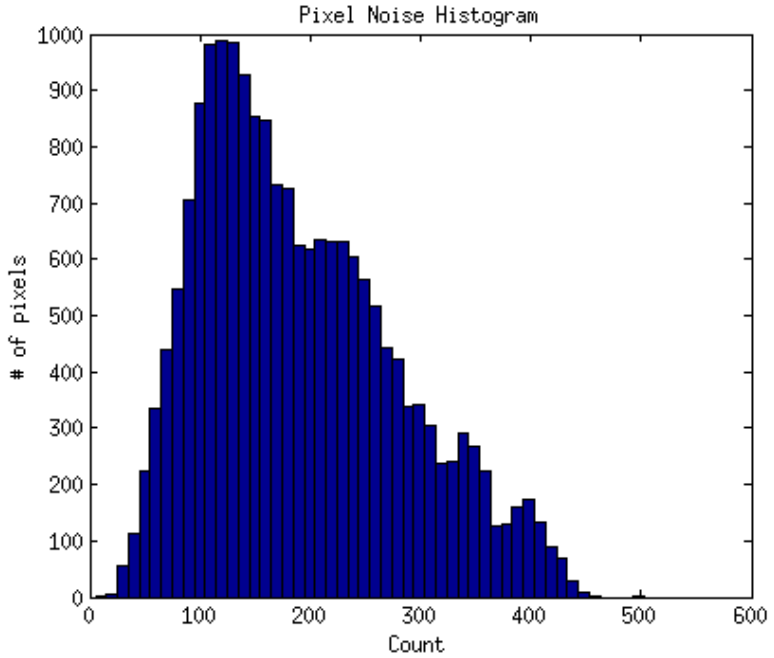


Figure 4.13: Detector noise histogram of the miniature camera with USB power. The average noise is 190 ADC count with 18-bit ADC which corresponds to 3.62m V_{RMS}.

Figure 4.14 shows an image taken with the 160x120 microbolometer with miniature camera.



Figure 4.14: An image taken with the 160x120 microbolometer with miniature camera.

Power dissipation of the miniature camera is also measured. The power consumption of the camera without the sensor is 0.1 Watts and with sensor is 0.2 Watts. Also, the digital interface and USB communication board has a power dissipation of 0.4Watts.

Total power dissipation of the miniature camera is 0.55 W with lens while power dissipation of the FLIR Quark is reported as less than 1 W [37]. The size of the miniature camera with housing and without lens is 29mm × 29mm × 18mm while size of the FLIR Quark camera is 22mm × 22mm × 17mm [37]. Table 4.2 shows the features of the miniature camera.

Table 4.2: Features of the miniature camera.

Features of the Miniature Camera	
Supply Powered Signal Chain Noise	19 μV_{RMS}
USB Powered Signal Chain Noise	23 μV_{RMS}
Supply Powered Zero Gain Noise	0.08 mV_{RMS}
USB Powered Zero Gain Noise	0.17 mV_{RMS}
Supply Powered Fixed Gain Noise	3.53 mV_{RMS}
USB Powered Fixed Gain Noise	3.62 mV_{RMS}
Size Without Housing	$2.9 \times 2.9 \times 1.8\ cm^3$
Size With Housing	$3.1 \times 3.1 \times 3.1\ cm^3$
Power Dissipation Without Sensor	0.5 Watts
Power Dissipation With Sensor	0.55 Watts

4.4 Conclusion

This chapter summarizes the test results of each camera. The noise levels resulted from three differentsources of the designed cameras are measured, separately. Firstly, noise of the analog signal block is measured. Analog signal block noise of the cameras consists of both the noise of the buffer and ADC. Secondly, zero-gain noise, i.e. the system noise independent from the noise induced by the pixels, is measured. Finally, the overall system noise with the sensor is measured.

Moreover, size, cost, and the power dissipation of each camera are summarized in this chapter. This chapter presents the effort on the optimization of noise, power dissipation, size, and cost of the each camera system. The test results shows that the desired ultra-small size is achieved without sacrificing the other performance parameters, noise, cost, and power dissipation.

CHAPTER 5

CONCLUSION AND FUTURE WORK

The research conducted in the scope of this thesis involves the design and development of camera electronics for uncooled microbolometer type infrared detectors. During this thesis work, two different camera systems are designed; portable and miniature.

The portable camera is designed to assemble camera electronics and infrared detector in a compact camera with small form factor, low cost, low noise, and low power system.

The miniature camera is a different concept of thermal cameras which can be used as an accessory to the portable systems such as cellular phones or tablets. During the design and realization of the miniature camera module, the challenges of reducing the volume of the system is studied and various problems are solved. The resulting miniature camera module is optimized to be USB powered and it can be connected directly to a host computer for data transfer. The realized miniature camera module in the scope of this thesis is one of the first examples of miniature infrared camera systems in the literature.

The major achievements of the thesis can be listed as follows:

1. The drawbacks of the previous works of the camera electronics are studied, and then the portable camera electronics are designed with areas of 7.5×5 cm^2. The overall module is powered by an external 6 V supply and directly connected to a host computer via USB interface. The test results of the realized portable camera module shows that the power dissipation of the overall camera module is less than 0.55 W and the system noise is less than 0.44mV_{RMS}.

2. A custom and application optimized digital interface and USB communicationboard is designed in order to minimize the cost of the portable camera electronics. This board can be powered up by either USB interface or an external power source.The power dissipation of this board is measured to be 0.4 W which is much less than the commercial FPGA boards with comparable specifications.

3. The miniature camera module is designed and developed to produce ultra-small size, low cost, and low power infrared camera systems. The size of the miniature camera boards are 2.9×2.9 cm^2.The module is powered by the USB interface and does not require any additional power sources. The test results of the realized miniature camera system shows that the power dissipation of the overall module is 0.6 W, and the system noise is less than 80 μV_{RMS}.The miniature camera module designed and realized in the scope of this thesis is the first miniature infrared camera module in Turkey. The developed camera modules can be used to produce very low cost and ultra-portable infrared camera systems.

The future works that need to be studied are summarized as follows:

1. Thermal images should be taken, when vacuum packaged uncooled thermal detectors are arrived.

2. Testability of the design camera electronics should be developed.

3. Built-in test structure should be designed.

REFERENCES

[1] Hamamatsu Photonics K.K., "Characteristics and Use of Infrared Detectors," Solid State division, Tokyo, Japan, 2004.

[2] http://en.wikipedia.org/wiki/Infrared, Last Access: August 21th, 2012.

[3] P. V. V. Jayaweera, "Uncooled Infrared Photon Detection Concepts and Devices," *Ph D Dissertation*, Georgia State University, 2009.

[4] T. Akın, "CMOS-based Thermal Sensors" in Advanced Micro &Nanosystems Volume 2: CMOS-MEMS, Edited by H. Baltes, O. Brand, G.K. Fedder, C. Hierold, J. Kornivk, O. Tabata, Wiley-VCH, 2005. AMN-Flyer

[5] T. J. Seebeck, "The Magnetic Polarization of Metals and Ores Produced by Temperature Difference," *Proc. of Prussian Acad. of Sciences*, pp 265–373, 1822.

[6] M. Y. Tanrıkulu, "An Uncooled Infrared Microbolometer Array Using Surface Micromachined MEMS Technology," *Ph.D. Dissertation*, Middle East Technical University, August 2007.

[7] M. Tepegöz, "A Monolithic Readout Circuit for Large Format Uncooled Infrared Detector Focal Plane Arrays," *M.S. Thesis*, Department of Electrical and Electronics Engineering, Middle East Technical University, 2010.

[8] D. S. Tezcan, S. Eminoğlu, and T. Akın, "A Low Cost Uncooled Infrared Microbolometer Detector in Standard CMOS Technology," *IEEE Transactions on Electron Devices*, Vol. 50, No. 2, pp. 494-502, 2003.

[9] E. Alpman, "Development of Low-Cost Uncooled Infrared Detector Arrays in Standard CMOS and SOI-CMOS Processes," *M.S. Thesis*, Department of Electrical and Electronics Engineering, Middle East Technical University, 2005.

[10] K. S. Demirci, "A Low-Cost 16x16 Uncooled Infrared Detector FPA Using Standard CMOS and Wafer Level MEMS Processes," *M.S. Thesis*, Department of Electrical and Electronics Engineering, Middle East Technical University, 2005.

[11] D. S. Tezcan, S. Eminoğlu, O. Akar, and T. Akın, "An Uncooled Microbolometer Infrared Focal Plane Array in Standard CMOS," *Proceedings of SPIE*, Vol. 4288, pp. 112-121, 2001.

[12] S. Eminoğlu, M. Y. Tanrıkulu, and T. Akın, "Low-Cost 64x64 Uncooled Infrared Detector Arrays in Standard CMOS," *The 12th Int. Conf. on Solid-State Sensors and Actuators (TRANSDUCERS'03)*, pp. 316-319, 2003.

[13] S. Eminoğlu, "Uncooled Infrared Focal Plane Arrays with Integrated Readout Circuitry Using MEMS and Standard CMOS Technologies," *Ph. D. Dissertation*, Department of Electrical and Electronics Engineering, Middle East Technical University, 2003.

[14] S. Eminoğlu, M. Y. Tanrıkulu, and T. Akın, "Low-Cost Uncooled Infrared Detector Arrays in Standard CMOS," *Proceedings of SPIE*, Vol. 5074, pp. 425-436, 2003.

[15] http://www.securitysales.com/files/advertise/ss7dumies.pdf, Last Access: December 5th2012.

[16] A. Rogalski, "History of Infrared Detectors," *Infrared Physics & Technology*, Vol. 43, pp. 187–210, 2002.

[17] P. Norton, "Third generation sensors for night vision," *Opto-Electronics Review*, Volume 14, Issue 1, pp 1-10, 2006.

[18] FLIR Systems Inc, "FLIR Infrared Cameras for SprayFoam Professionals," 2010.

[19] P. W. Kruse and D. D. Skatrud, "*Uncooled Infrared Imaging Arrays and Systems*", Semiconductor and Semimetals, Vol. 47, Academic Press, 1997.

[20] D. Akçören, "A Low-Cost Uncooled Infrared Detector Array and Its Camera Electronics," *M.S. Thesis*, Department of Electrical and Electronics Engineering, Middle East Technical University, 2011.

[21] E. İncetürkmen, "A Low-Cost 128x128 Uncooled Infrared Detector Array in A Standard SOI CMOS Technology," *M.S. Thesis*, Department of Electrical and Electronics Engineering, Middle East Technical University, 2008.
[22] M. B. Dayanık, "Low-Cost High Performance Infrared Detectors in SOI-CMOS Technology," *M.S. Thesis*, Department of Electrical and Electronics Engineering, Middle East Technical University, 2007.
[23] Mikrosens, "MS1670 Datasheet," 2012.
[24] http://www2.engr.arizona.edu/~ece372_spr04/ece372_spr05/References/pcb_ xilinx.pdf, Last Access: September 15th, 2012.
[25] Analog Devices, "Printed Circuit Board (PCB) Design Issues," in *Basic Linear Design*, Edited by H. Zumbahlen, 2007.
[26] C. Hollitt, "Printed Circuit Board Design,"*ECEN303/PHYS341 Analogue Electronics*, Victoria University of Wellington, July 2012.
[27] Frescale Semiconductor, "High Speed Layout Design Guidelines," Application Note, Rev. 2, 2006.
[28] Altera, "Minimizing Ground Bounce &Vcc Sag," White Paper, 2001.
[29] M. Defossez, "Selecting Connectors for Multi-Gigabit Transceiver Designs", Xilinx, 2005.
[30] http://www.ece.unm.edu/~jimp/650/slides/connectors1.pdf, Last Access: November 19th 2012.
[31] J. Axelson, "USB Complete: Everything You Need to Develop USB Peripherals," Third Edition, Lakeview Research LCC, 2005.
[32] TXC Corporation, "TS809CXD Datasheet".
[33] C. Vieider, S. Wissmar, P. Ericsson, U. Halldin, F. Niklaus, G. Stemme, J. E. Källhammer, H. Pettersson, D. Eriksson, H. Jakobsen, T. Kvisterøy, J. Franks, J. VanNylen, H. Vercammen, and A. VanHulsel., "Low-Cost Far Infrared Bolometer Camera for Automotive Use", *Proceedings of SPIE*, Vol.6542, pp.1L.1-1L.10, Orlando, 2007.
[34] FLIR, "Cooled versus Uncooled Cameras for Long Range Surveillance," Technical Note.
[35] Umicore, "GASIR Standard Assembly FL 8.5 mm f/1.2 Datasheet".
[36] T. Akın, Z. Olgun, and H. Külah, "An Integrated Thermopile Structure with High Responsivity Using any Standard CMOS Process," *Sensors and Actuators*, pp. 218-224, 1998.
[37] FLIR Systems Inc, "FLIR Quark Brochure," 2011.
[38] F. Faccio, P. Aspell, P. Jarron, and E. H. Heijine, "An Additional Contribution in the Noise Spectrum of SOI MOSFETs", Proceedings *of IEEE International SOI Conference*, Oct. 1996.
[39] Mikrosens, "Thermal Imaging Applications," *Internal Document*, 2012.